Ecole de Métallurgie Fondamentale

Action Nationale de Formation (ANF)

22-25 Octobre 2012, Aussois

Métaux et Alliages sous Irradiation

P. Pareige
Groupe de Physique des Matériaux
UMR CNRS 6634, Université et INSA de Rouen

A. Barbu, B. Radiguet
SRMP, CEA Saclay
CIEMAT, Espagne
EDF, Les Renardières
...

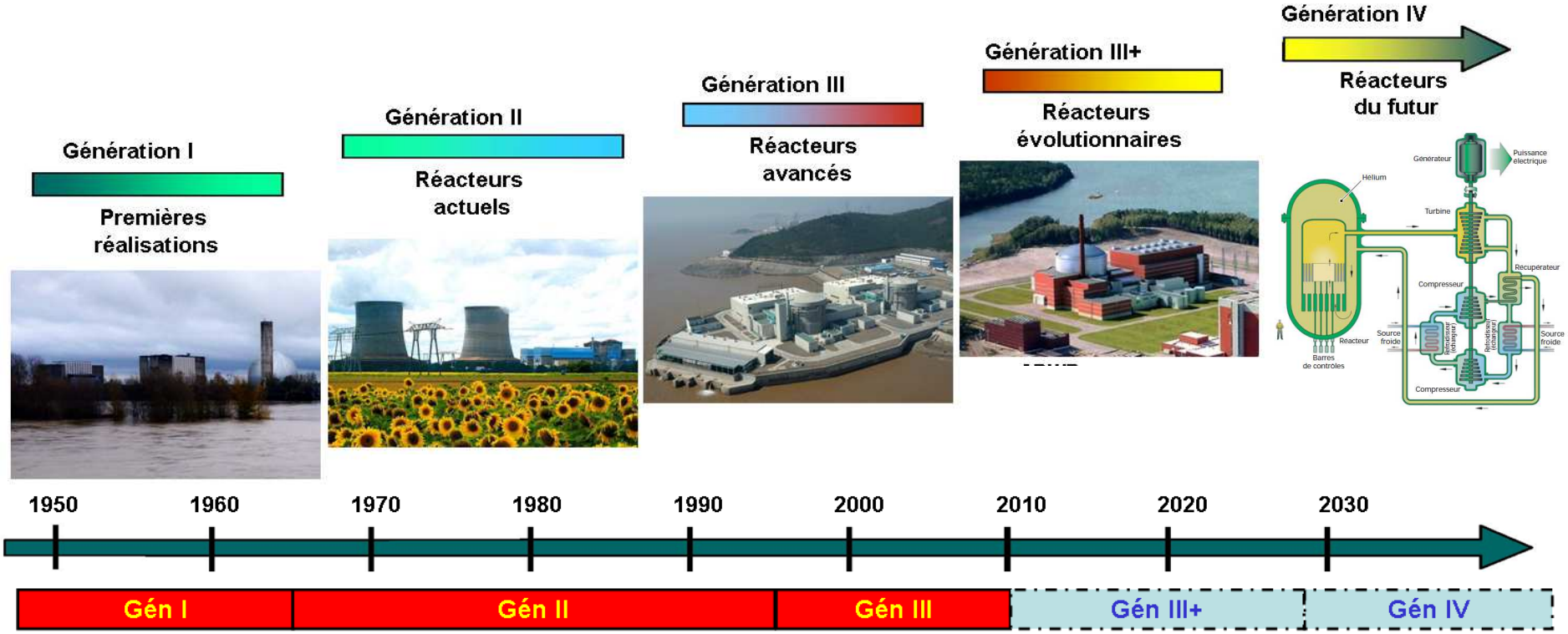

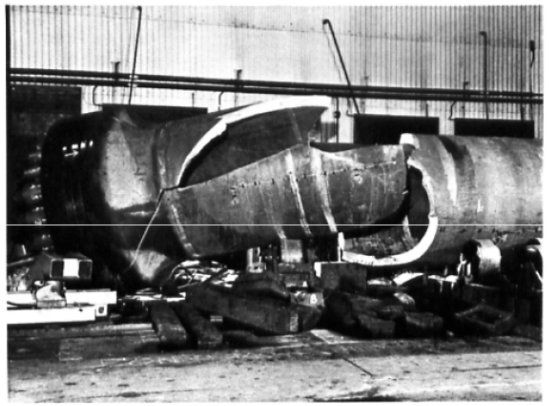

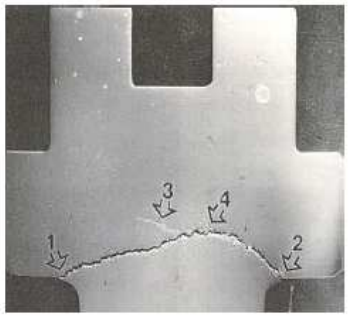

Fig. 1.12. *Failure by brittle fracture of thick-walled cylindrical pressure vessel during hydraulic test (By courtesy of John Thompson Ltd., Wolverhampton)*

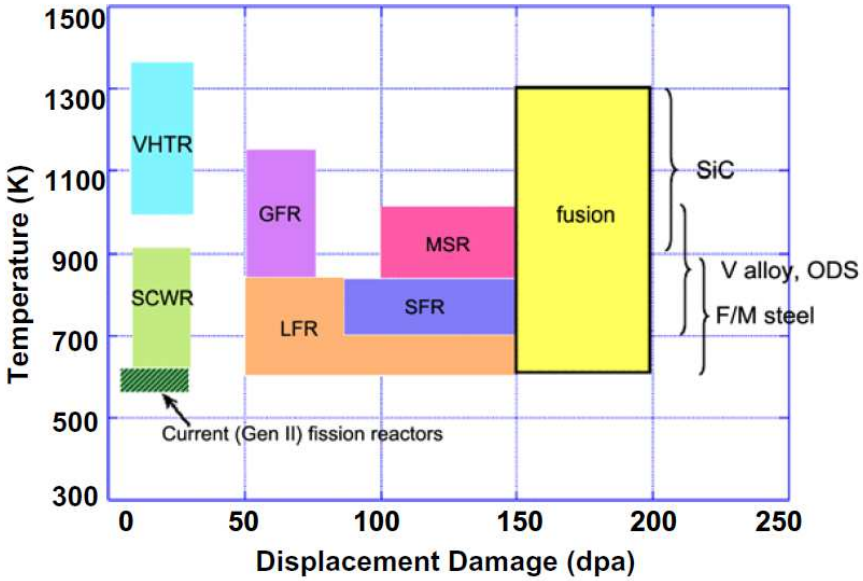

Outline

Interaction ion-matter

Ballistic Damage (primary damage)
- Frenkel pairs
- Atomic Displacement Cascade
- Disorder induced by ballistic damage

Properties of point defects and their clusters :
- Structure
- Mobility

Slow evolution (secondary damage) :
- Evolution of the point defects population:
- Consequence of the super-saturation of point defects
  - Agglomeration of point defects
  - Enhanced phase transformation
  - Induced Segregation and precipitation

Macroscopic Consequences

Outline

Interaction ion-matter

Ballistic Damage (primary damage)
- Frenkel pairs
- Atomic Displacement Cascade
- Disorder induced by ballistic damage

Properties of point defects and their clusters :
- Structure
- Mobility

Slow evolution (secondary damage) :
- Evolution of the point defects population:
- Consequence of the super-saturation of point defects
  - Agglomeration of point defects
  - Enhanced phase transformation
  - Induced Segregation and precipitation

Macroscopic Consequences

Origine du dommage d'irradiation: collision élastique

Neutron ➔ Chocs élastiques avec les noyaux

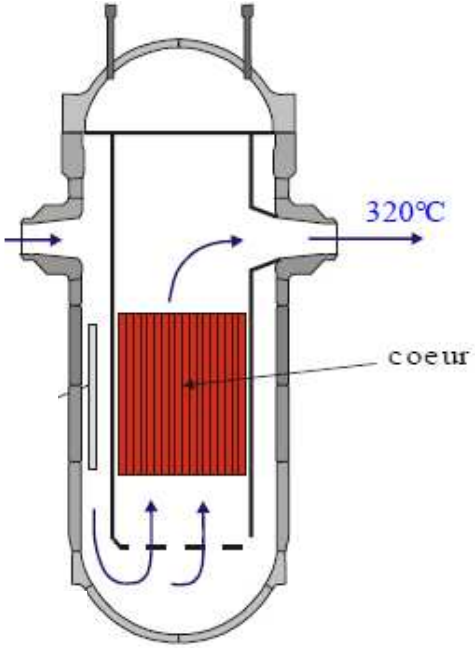

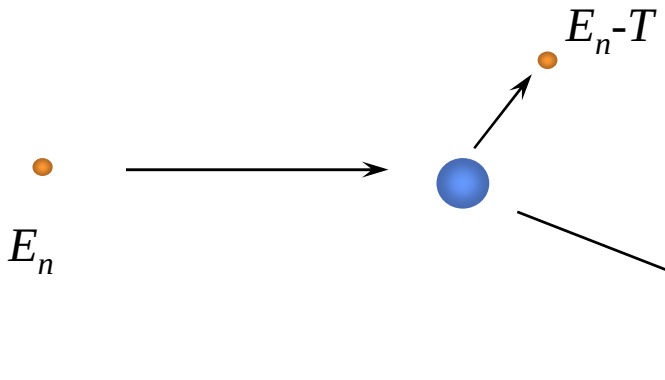

Primaire
(*PKA (primary knock-on atom)*)

$$\overline{T} = \frac{T_{Max}}{2}$$

$$T_{Max} = 4\frac{m_n.m_c}{(m_n + m_c)^2}E_n$$

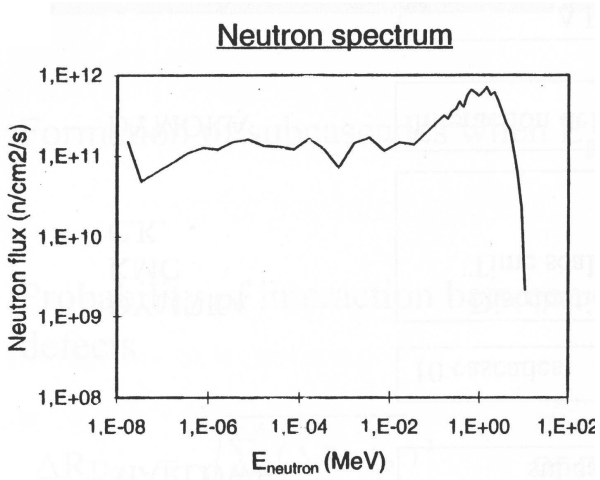

Ex: neutron de 1 MeV

sur un atome de fer

T_{max} ~ 70 keV

<T> ~ 35 keV

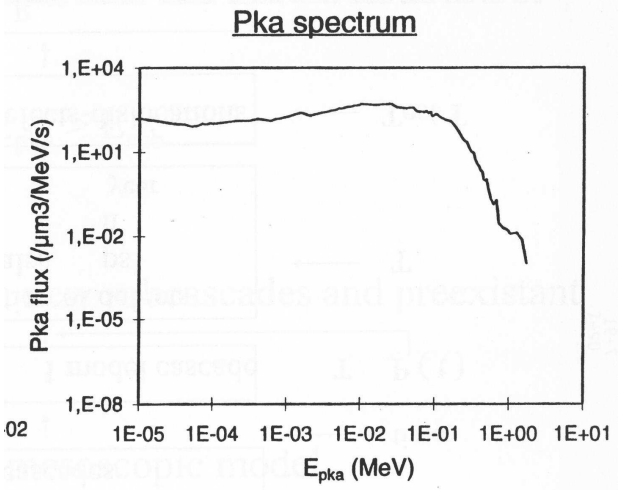

Interaction Ions-Métal

Collisions Elastique et Inélastique

Energy loss per unit path

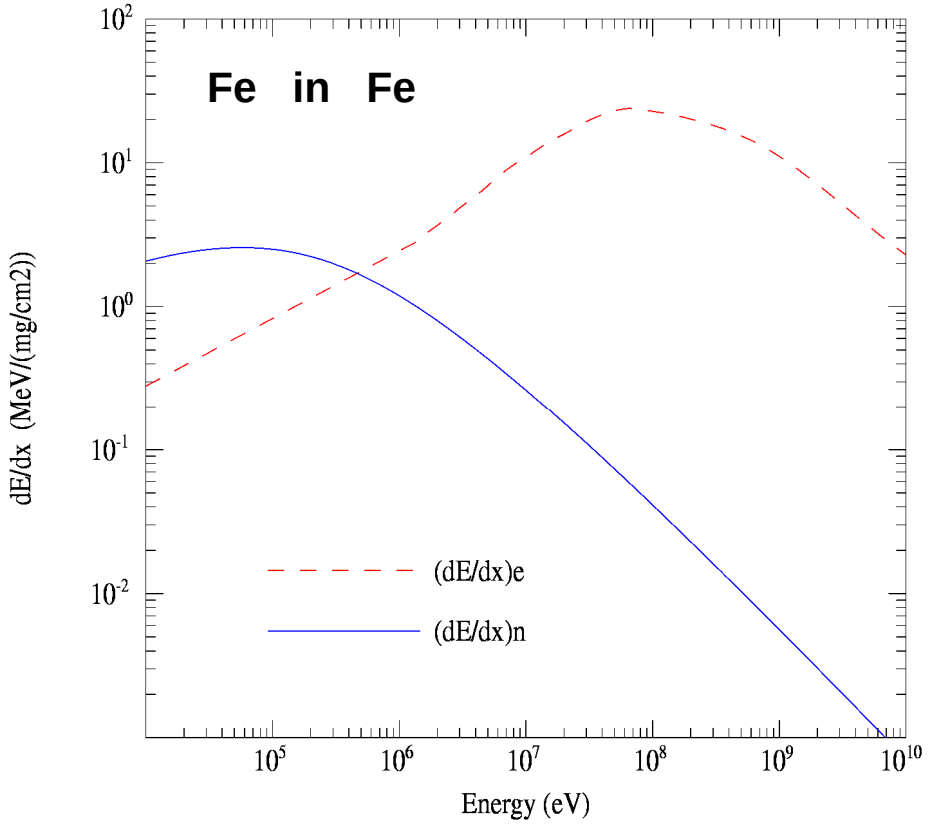

Stopping and Ranging of Ions in Matter (SRIM)

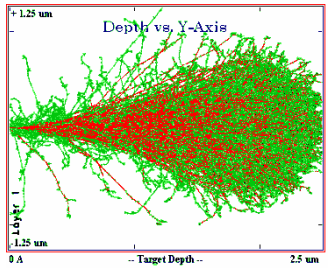

2.5 µm

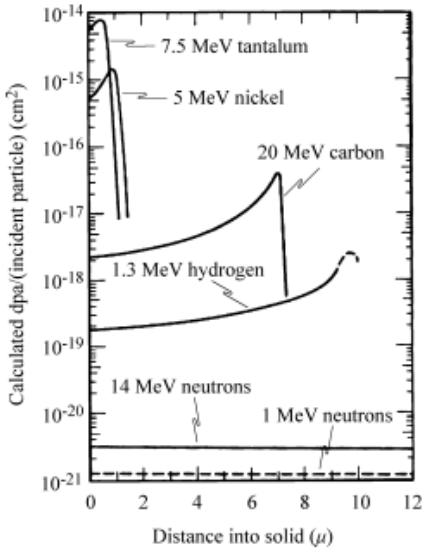

Dommage ballistique : seuil de déplacement

$\mathbf{E_d}$ = displacement threshold

1/ **T < E_d** : Phonon – Recombination

2/ **T > E_d but is low** : single **Frenkel pair**
(one vacancy + one interstitial)

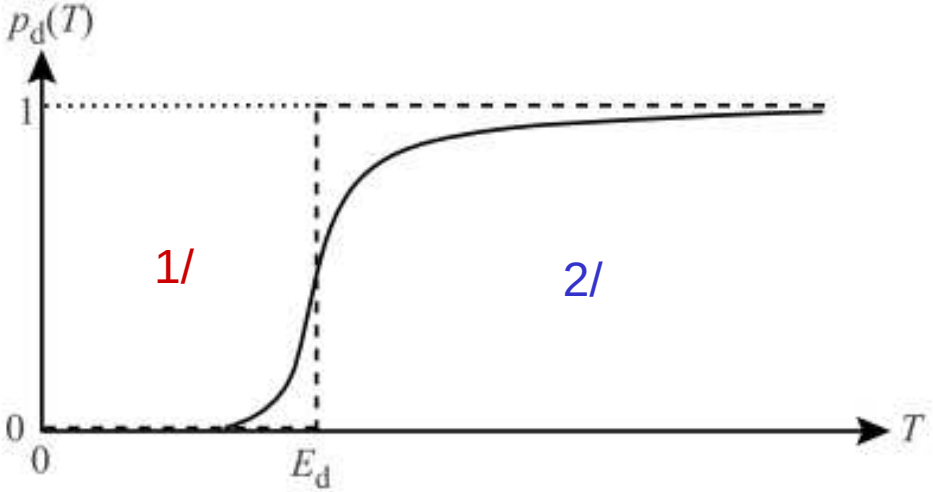

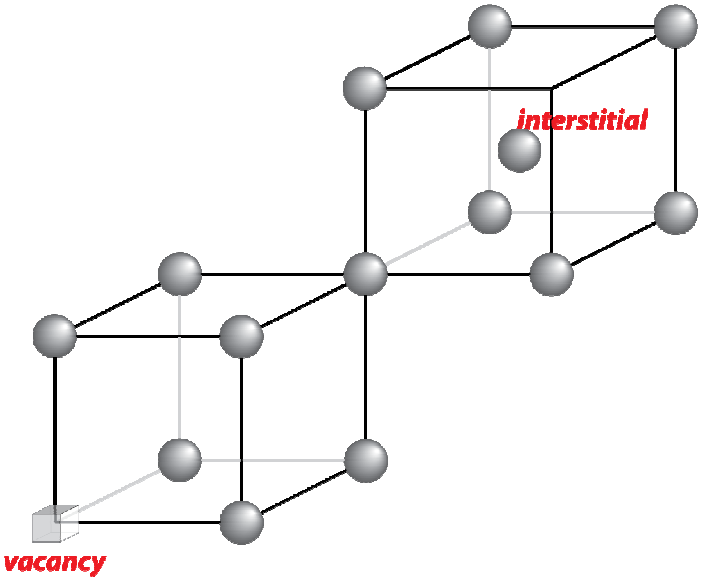

Dommage ballistique : seuil de déplacement

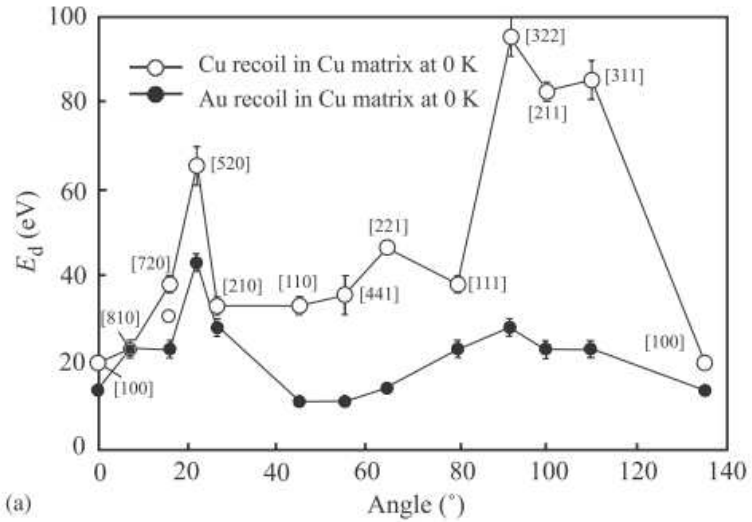

(a)

Metal	Lattice (c/a)	$E_{d,min}$ (eV)	E_d (eV)
Al	fcc	16	25
Ti	hcp (1.59)	19	30
V	bcc	–	40
Cr	bcc	28	40
Mn	bcc	–	40
Fe	bcc	20	40
Co	fcc	22	40
Ni	fcc	23	40
Cu	fcc	19	30
Zr	hcp	21	40
Nb	bcc	36	60
Mo	bcc	33	60
Ta	bcc	34	90
W	bcc	40	90
Pb	fcc	14	25
Stainless steel	fcc		40

Dommage ballistique : cascade de déplacements

3/ If $T>>E_d$ Atomic displacement cascade

Modèle de Kinchin-Pease

1- Cascade = suite de collisions à 2 corps (sphères dures)

2- $P_d(T) = 1$ si $T > E_d$ et 0 sinon

3- Pas d'énergie transférée au réseau ou sous forme d'excitation électronique

4- si $T > E_c$, pas de défauts supplémentaires

5- Arrangement aléatoire des atomes

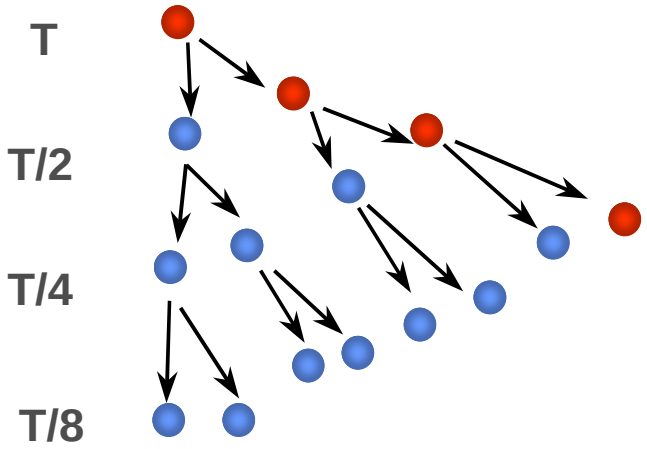

.... As far as $E > E_d$

Number of displaced atoms (Frenkel pairs) :

$T < E_d$	$\mathbf{N_d = 0}$
$E_d < T < 2\,E_d$	$\mathbf{N_d = 1}$
$2\,E_d < T < E_c$	$\mathbf{N_d = T/(2.E_d)}$
$T > E_c$	$\mathbf{N_d = E_c/(2.E_d)}$

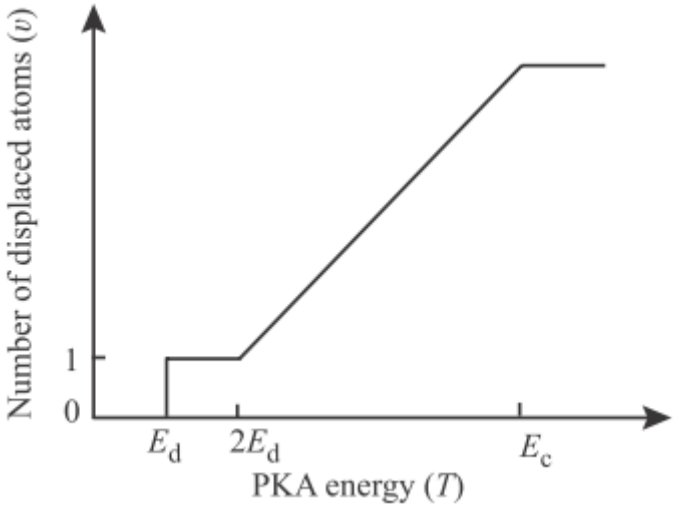

Dommage ballistique : cascade de déplacements

Modèle de Norgett, Robinson, Torrens (NRT)

- Potentiel d'interaction plus réaliste
- Excitation électronique

$$N_d = \frac{\kappa E_D}{2E_d} = \frac{\kappa(T-\eta)}{2E_d}$$

→ Efficacité de déplacement (κ):

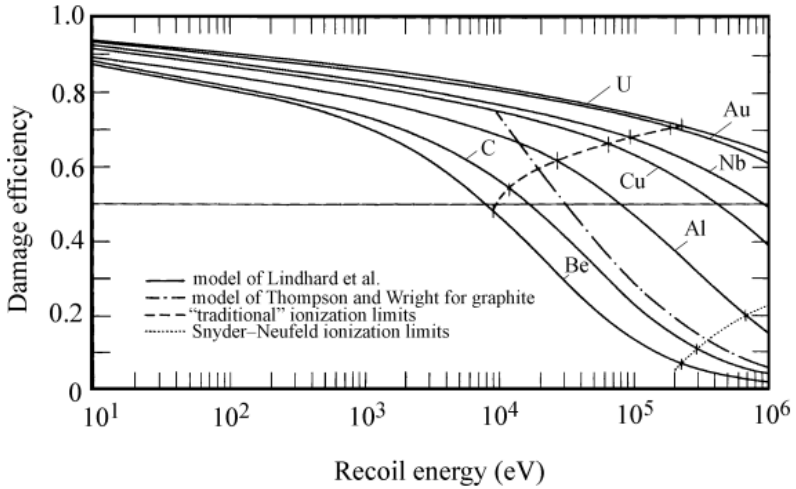

→ Energie de dommage (E_D):

T : énergie total du PKA
η: énergie perdue par excitation électronique dans la cascade

NRT

Number of displaced atoms

$T < E_d$	$N_d = 0$
$E_d < T < 2{,}5\ E_d$	$N_d = 1$
$2{,}5\ E_d < T < E_c$	$N_d = E_D/(2.E_d)$

Dommage ballistique : cascade de déplacements

Autre moyen d'étudier la cascade de déplacement : la modélisation : dynamique moléculaire

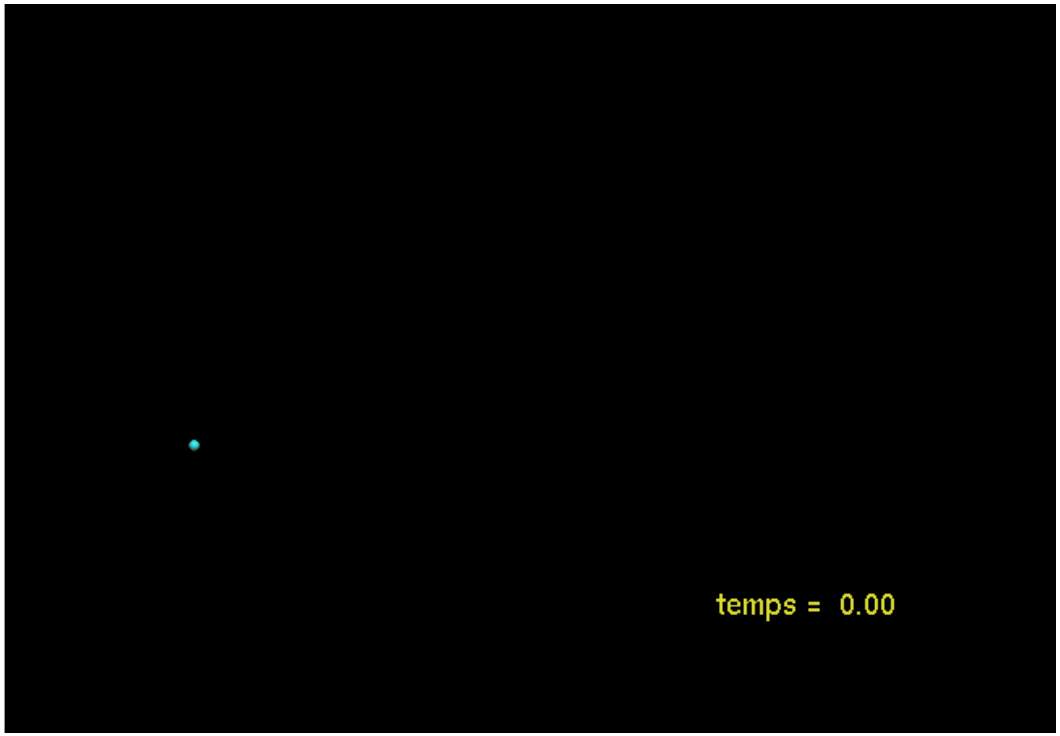

Sim. Dynamique Moléculaire: CEA Saclay

$$\frac{d^2 \vec{r}_i}{dt^2} = m_i^{-1}\left(-\frac{\partial E}{\partial \vec{r}_i}\right)$$

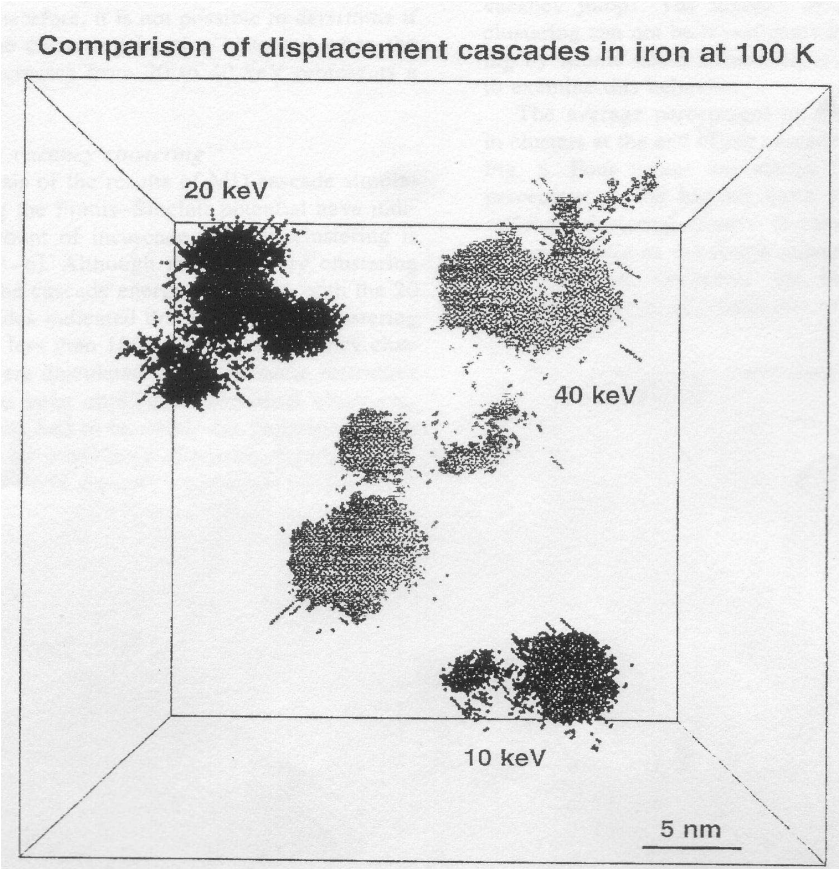

[R. E. Stoller, JNM, 1997]

Formation de sous cascades à haute énergie

Dommage ballistique : cascade de déplacements

4 keV Displacement cascade in Iron
Molecular Dynamic Simulation (C. Domain - EDF)

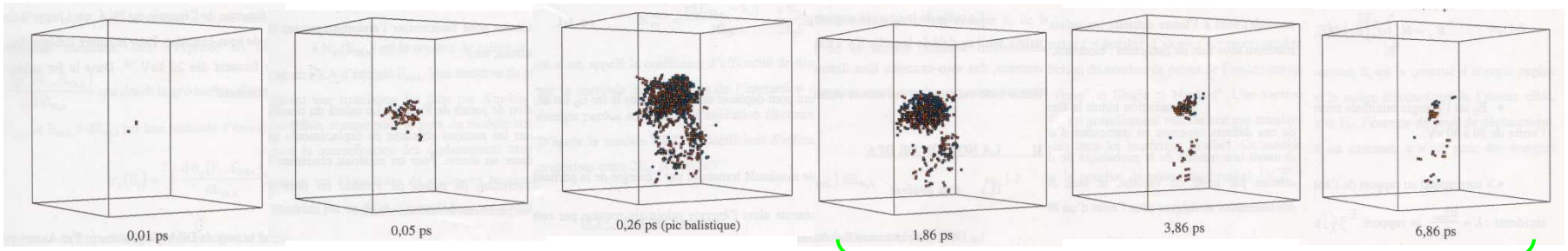

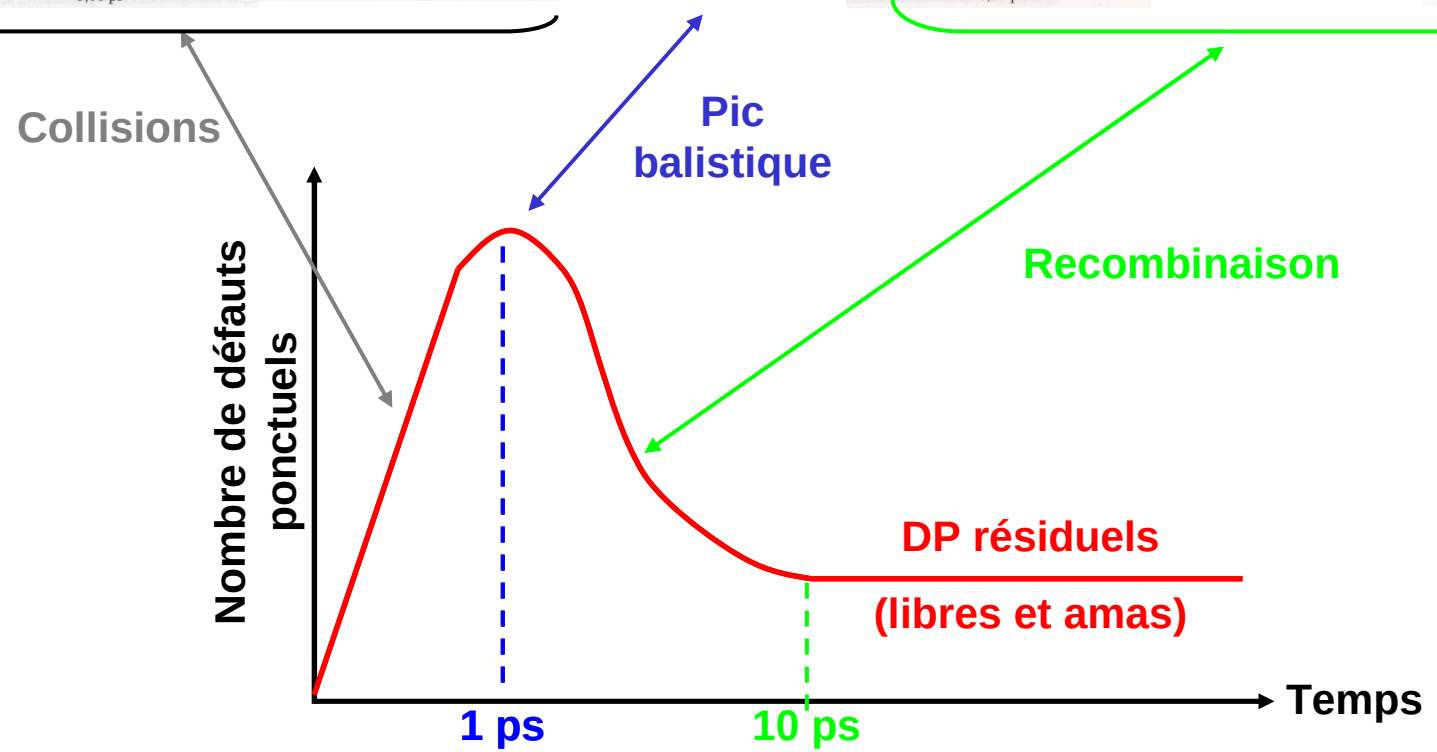

Qu'est ce qu'un résidu de cascade….?

Cascade in Fe, 10 ps after the collision
Pka of 20 keV.
Molecular Dynamic Simulation

Remains after 10 ps
- **isolated Interstitials.**
- **isolated vacancies.**
- **Clusters of interstitials.**
- **Clusters of vacancies.**

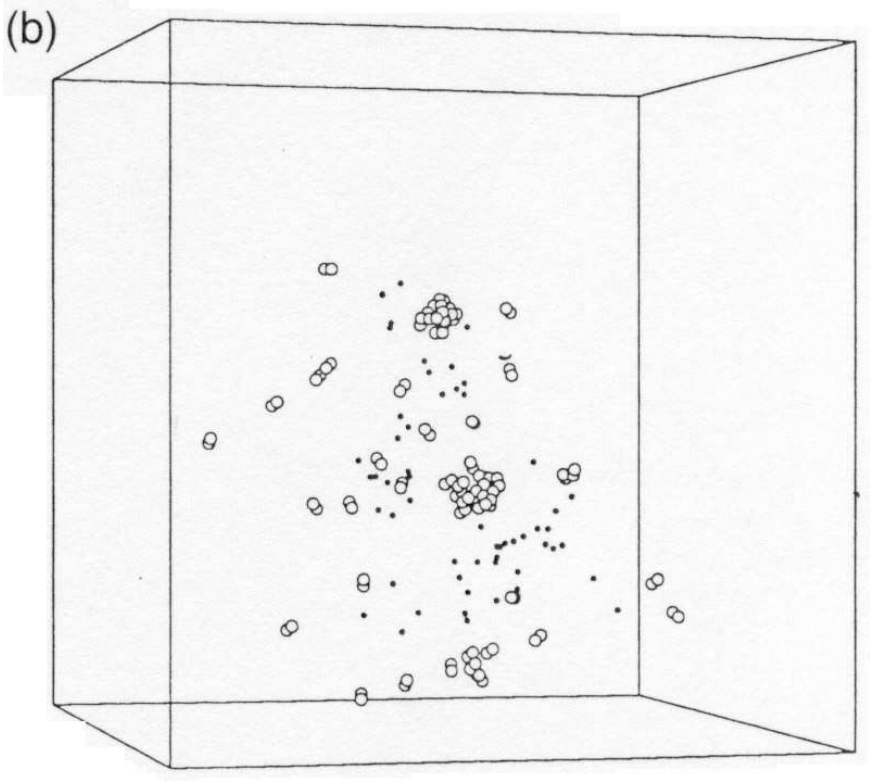

Défauts ponctuels et amas de défauts ponctuels dans les résidus

distribution of interstitial and vacancy clusters in cascades induced by primary iron ions (1 to 30 keV) in Fe (Vascon 1997)

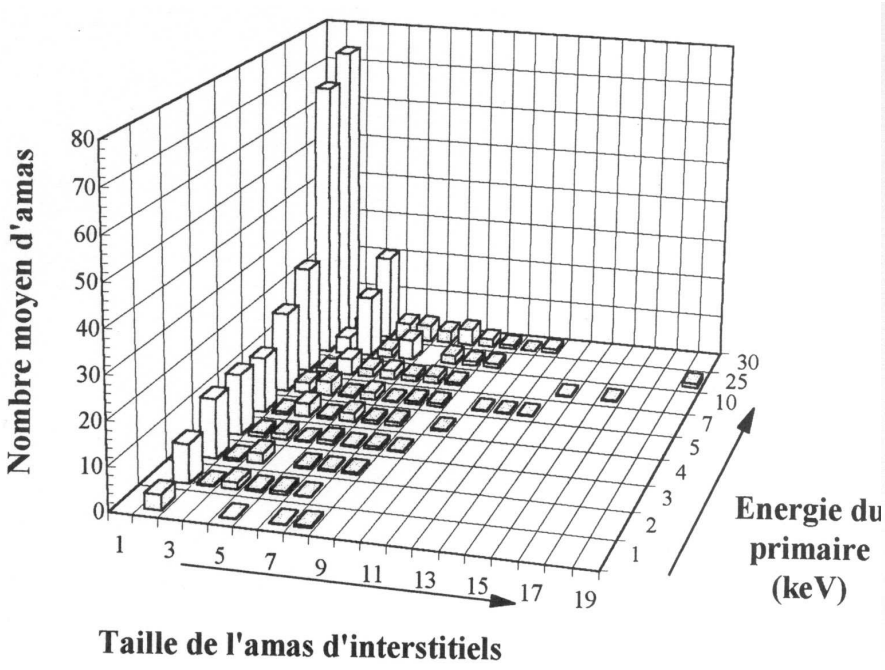

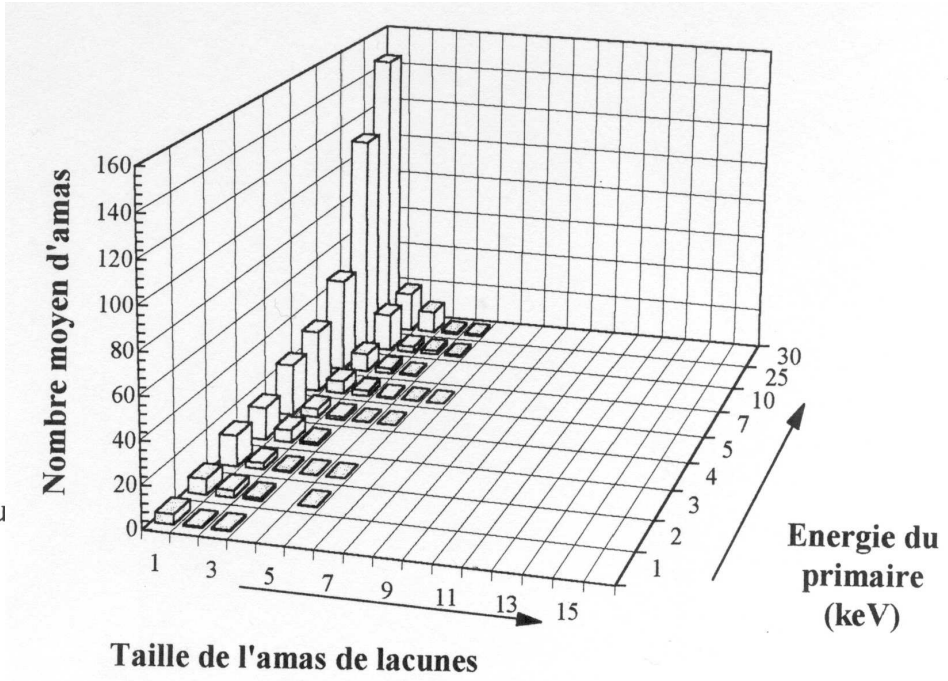

A large portion of point defects is in the form of clusters

dpa DM versus dpa NRT

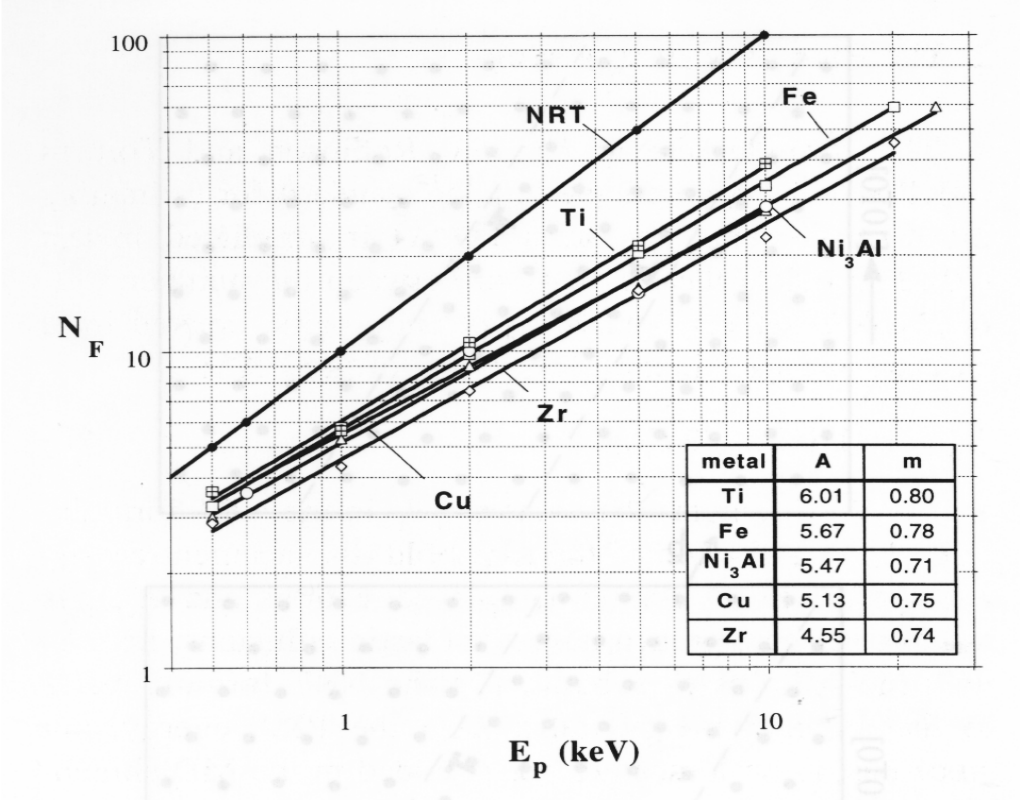

metal	A	m
Ti	6.01	0.80
Fe	5.67	0.78
Ni_3Al	5.47	0.71
Cu	5.13	0.75
Zr	4.55	0.74

Le nombre de dpa donné par la dynamique moléculaire (DM) nettement inférieur aux dpa NRT

Quelques ordres de grandeur des taux de dommage

Réacteurs

	Flux neutrons $m^{-2}s^{-1}$ (n>1MeV)	dpa_{NRT}/s	dpa_{NRT} fin de vie	T °C	Pb associés
REP éléments de coeur	10^{17}	$3\ 10^{-8}$	qqs dpa	≤ 400	**Internes** : corrosion sous contrainte assistée par l'irradiation **gaines** : fluage, croissance, corrosion
REP Cuve	10^{15}	$3\ 10^{-10}$	0.2	290	Fragilisation
RNR gaines	$3\ 10^{18}$	10^{-6}	150	550	Gonflement

Particules chargées

Accélérateur d'ions	10^{-3} - 10^{-5} dpa_{NRT}/s
Microscope électronique à haute tension (électrons)	10^{-3} - 10^{-5} dpa_{NRT}/s
Accélérateur d'électrons	10^{-9} dpa_{NRT}/s

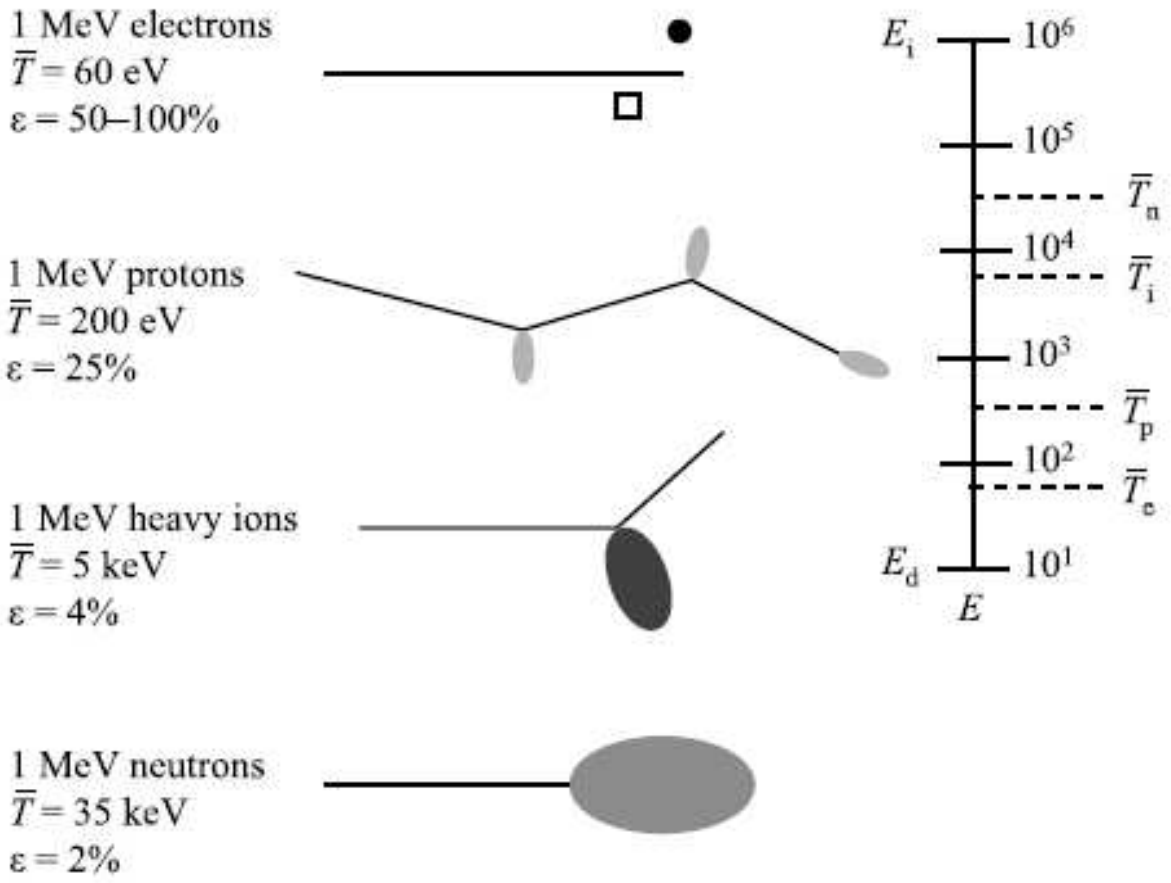

Fig. 3.7. Difference in damage morphology, displacement efficiency and average recoil energy for 1 MeV particles of different type incident on nickel (after [6])

Effet du dommage ballistique: Désordre chimique

Disorder

May be kept and observed at low temperature

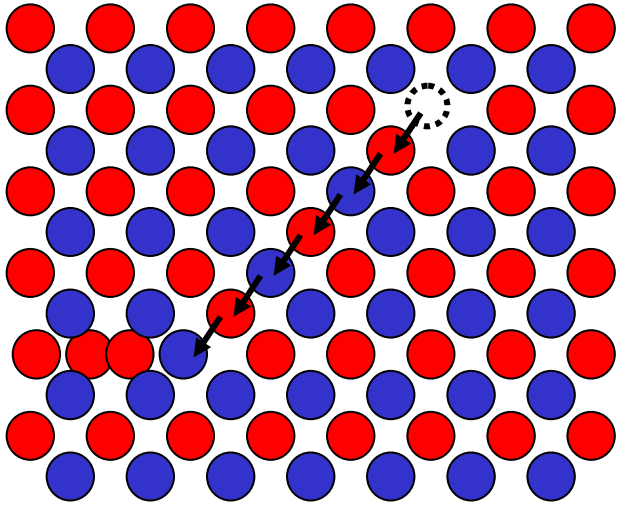

Crowdion
=
chemical disorder in ordered alloys

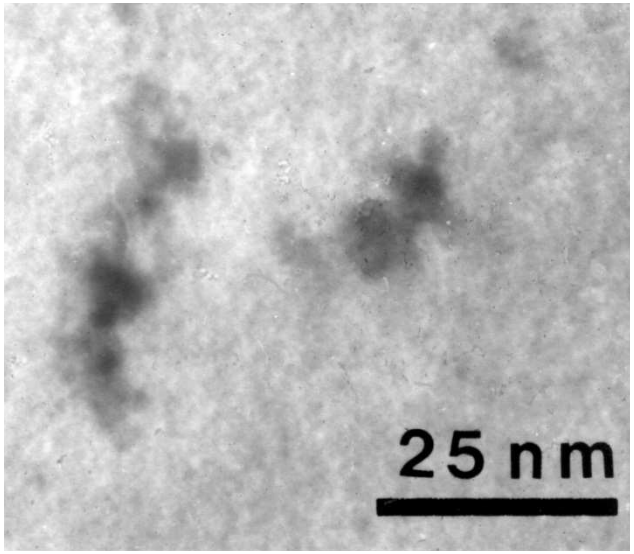

Disordered areas induced
by displacement cascades
in an ordered Cu_3Au alloy

Effet du dommage ballistique: Amorphisation

Lost of the crystalline structure in the cascade, for some compounds

Amorphisation under irradiation of $Zr(Fe,Cr)_2$ precipitate in Zircaloy (Fe back to solution).

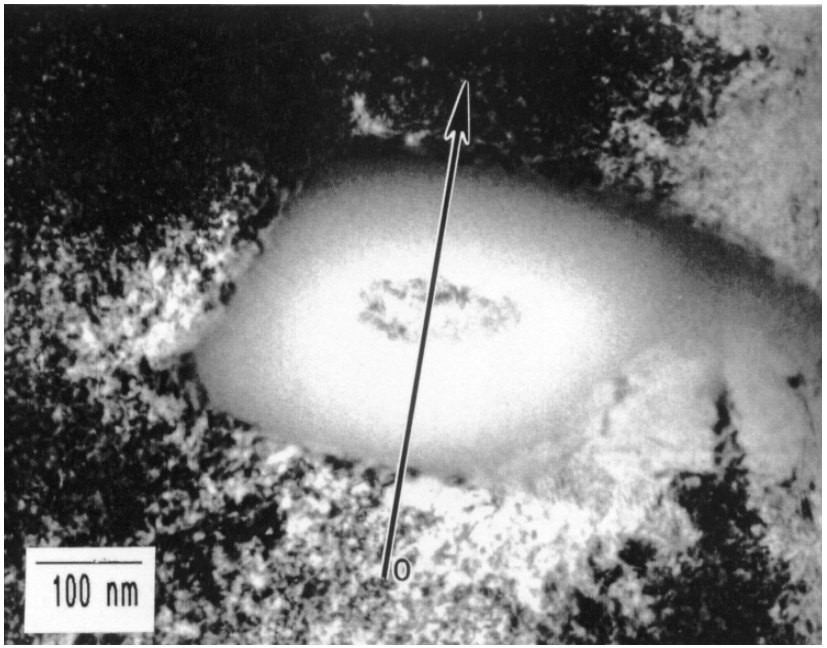

Cascades versus thermodynamique

Approximation

an alloy with clustering tendency will achieve under irradiation the macro state it would have outside irradiation at a higher effective temperature T_{eff}

$$T_{eff} = T\left(1 + \frac{D^{bal}}{D_{ch}}\right)$$

In alloy with ordering tendency, owing to the flux and temperature : enhancement of the ordering kinetic of a disordered solid solution (quenched) or disordering of an ordered alloy.

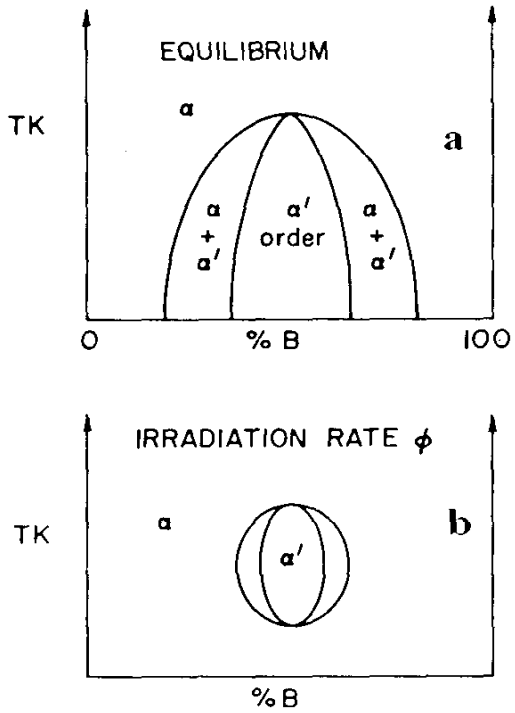

Modification of the phase diagram

Wilkes 1979

Outline

Interaction ion-matter

Ballistic Damage (primary damage)
- Frenkel pairs
- Atomic Displacement Cascade
- Disorder induced by ballistic damage

Properties of point defects and their clusters :
- Structure
- Mobility

Slow evolution (secondary damage) :
- Evolution of the point defects population:
- Consequence of the super-saturation of point defects
  - Agglomeration of point defects
  - Enhanced phase transformation
  - Induced Segregation and precipitation

Macroscopic Consequences

Structure des défauts ponctuels

Interstitial

In compact structures (metals), for **Self Interstitial Atoms** (SIA), the stable configuration is N atoms sharing the same crystallographic site (**dumbbell** or **crowdion**) configuration.

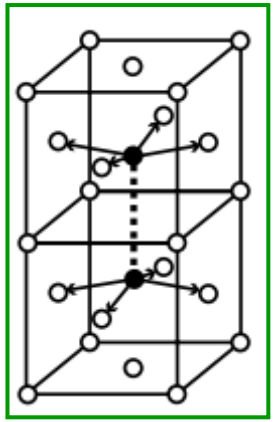

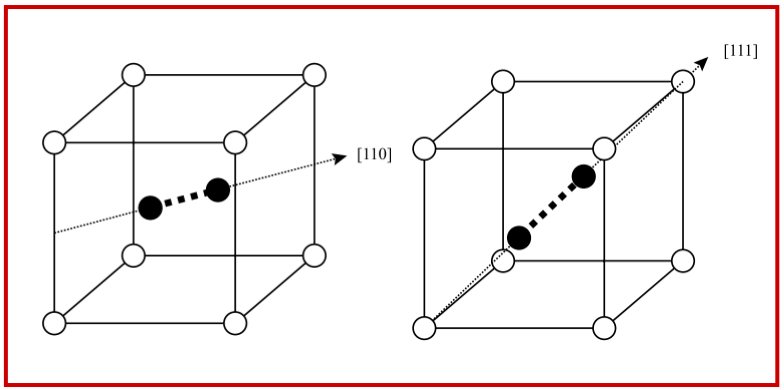

Energy of formation (E^f_I): **3 to 5 eV**

Relaxation Volume (V^r_I): **high** (~1.5 Ω)

Vacancy

= empty crystallographic site

FCC

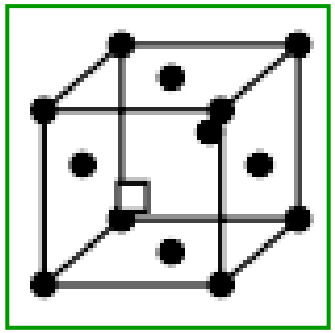

BCC

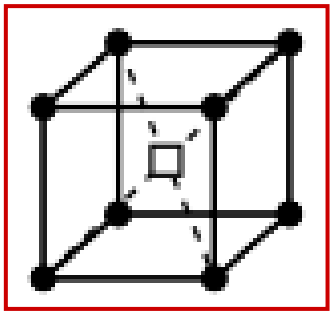

Energy of formation **(E^f_v) :** **0.6 to 2 eV**
Relaxation Volume **(V^r_v) :** **weak** (-0.2 Ω)

Point defects and small clusters

Di-Interstitials

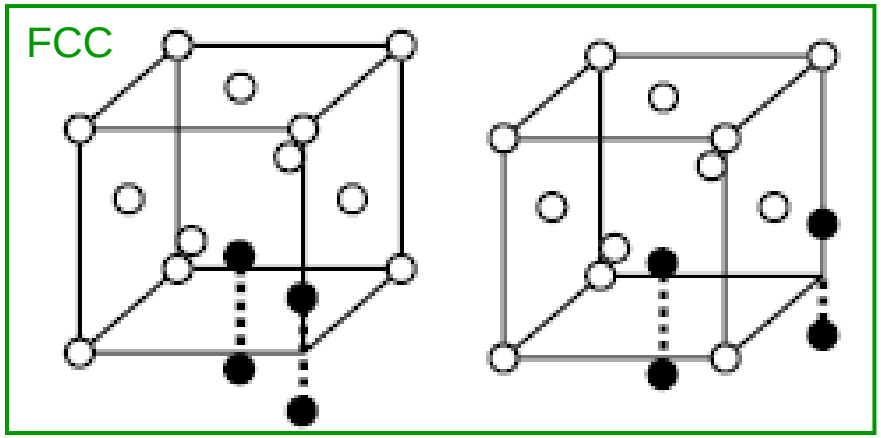

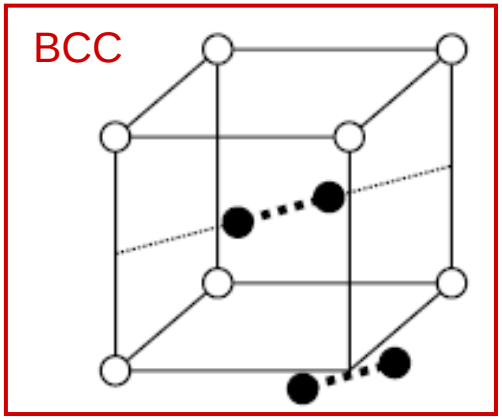

Di- and tri-vacancies

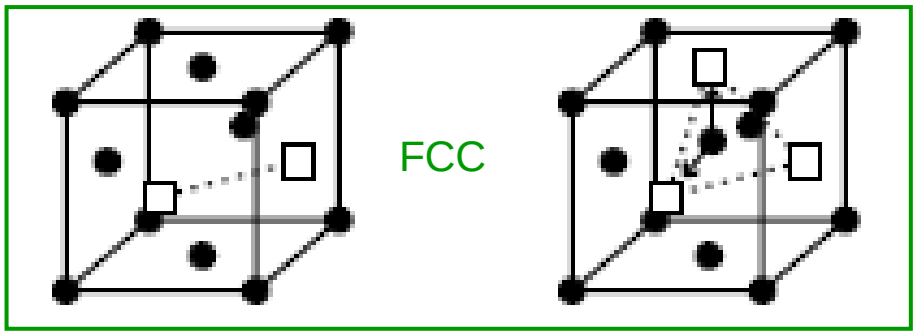

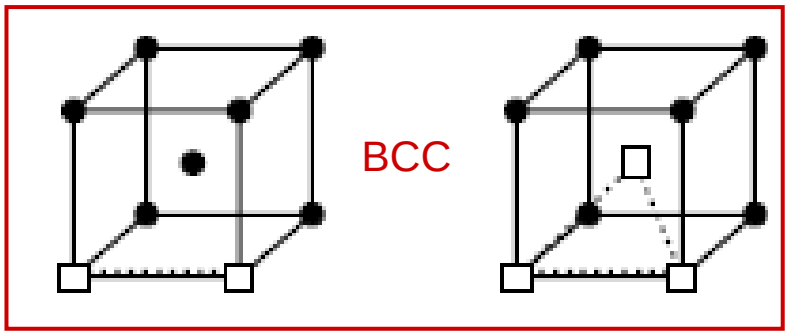

SIA dans Fe-α

Configurations

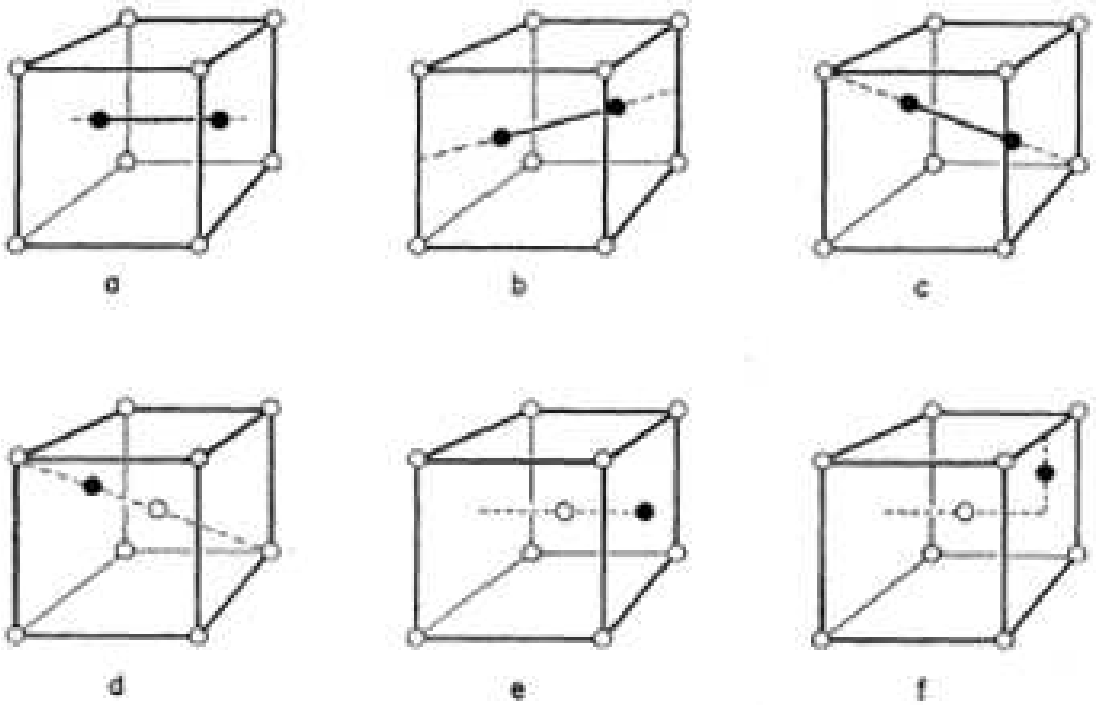

a) <100> dumbbell
b) <110> dumbbell
c) <111> dumbbell
d) <111> crowdion
e) interstitiel octaédrique
f) interstitiel tétraédrique

SIA dans Fe-α

Energie de formation des différentes configurations

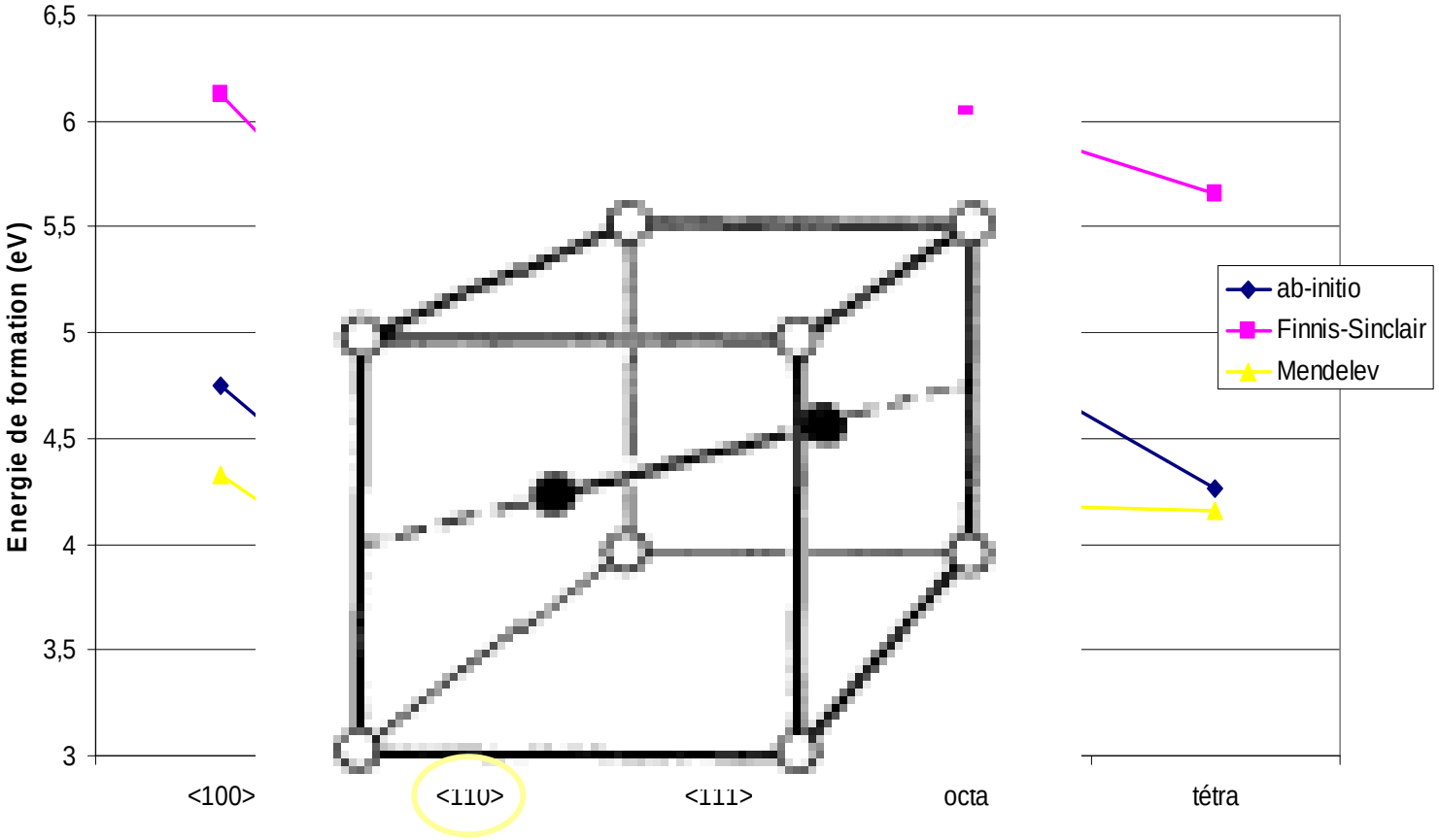

Configuration la plus stable <110> dumbbell

SIA dans Fe-α

Mécanismes de migration

- Mécanisme de rotation/translation (DM)

  - Rotation <110> ⇒ crowdion

  (0,13 < E_m < 0,25 eV)

  - Translation <111> (≈ 0,04 eV)

- Mécanisme de Johnson (Ab-initio)

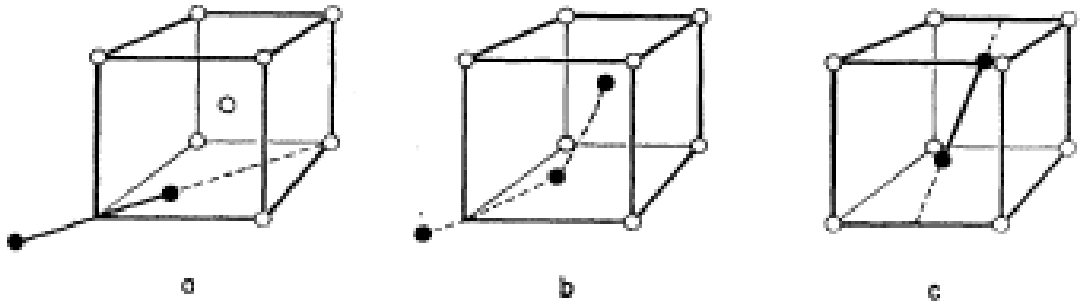

<110> centré en (0,0,0) ⇒ <101> centré en (1/2,1/2,1/2)

(≈ 0,30eV)

Amas d'interstitiels dans Fe-α

Configuration

- n < 5 :
  - ab-initio : ensemble de dumbbells <110> parallèles

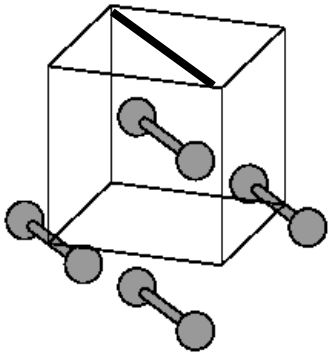

Tétra-interstitiel <110> dumbbells

E_f = 11,05 eV

  - DM : ensemble de crowdions <111> parallèles

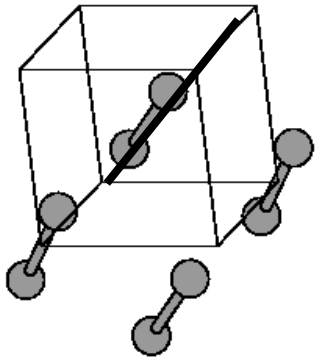

Tétra-interstitiel <111> crowdions

E_f = 14,4 eV (Wirth avec potentiel d'Ackland)

Amas d'interstitiels dans Fe-α

Configuration

• n ≥ 5 :

- ab-initio et DM : ensemble de crowdions <111> parallèles

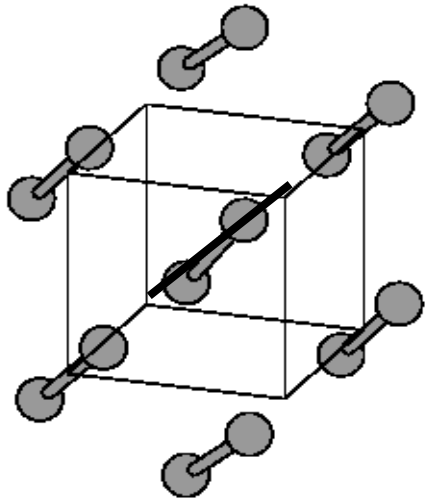

Hepta-interstitiel <111> crowdions

Ab-initio: E_f = 16,6 eV

DM : E_f = 21,1 eV
(Soneda avec potentiel de Johnson)

Travaux récents : C15 Laves structure

PRL 108, 025501 (2012) PHYSICAL REVIEW LETTERS week ending 13 JANUARY 2012

Irradiation-Induced Formation of Nanocrystallites with *C*15 Laves Phase Structure in bcc Iron

M.-C. Marinica, F. Willaime,* and J.-P. Crocombette

CEA, DEN, Service de Recherches de Métallurgie Physique, F-91191 Gif-sur-Yvette, France

(Received 28 September 2011; revised manuscript received 22 November 2011; published 11 January 2012)

A three-dimensional periodic structure is proposed for self-interstitial clusters in body-centered-cubic metals, as opposed to the conventional two-dimensional loop morphology. The underlying crystal structure corresponds to the *C*15 Laves phase. Using density functional theory and interatomic potential calculations, we demonstrate that in α-iron these *C*15 aggregates are highly stable and immobile and that they exhibit large antiferromagnetic moments. They form directly in displacement cascades, and they can grow by capturing self-interstitials. They thus constitute an important new element to account for when predicting the microstructural evolution of iron base materials under irradiation.

DOI: 10.1103/PhysRevLett.108.025501 PACS numbers: 61.72.Bb, 61.72.jj, 61.80.Az, 61.82.Bg

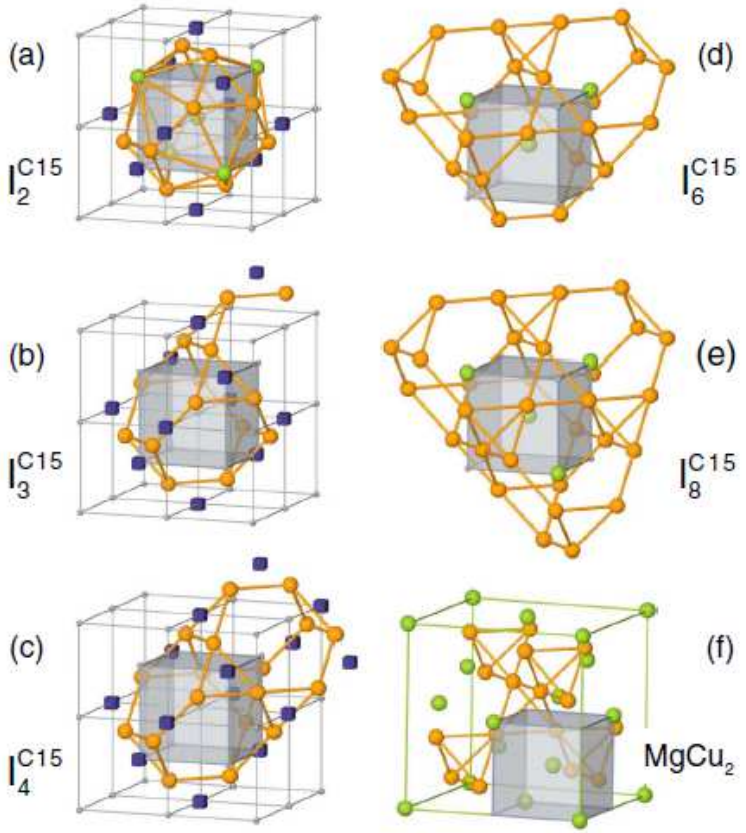

FIG. 1 (color online). Structure of small *C*15 interstitial clusters in the bcc lattice. (a)–(c) Representation by vacancies (blue cubes) and interstitials (orange spheres) of the di-, tri-, and tetra-interstitial clusters. For the di-interstitial, the atoms of the bcc lattice at the center and at the edges of the *Z*16 Frank-Kasper polyhedron are also represented (green spheres). (d),(e) Skeleton representation, i.e., without the vacancies and the cubic lattice and with the atoms at the center of the *Z*16 polyhedra in green, of the hexa- and octa-interstitials. (f) Unit cell of the $MgCu_2$ *C*15 Laves structure, with the Mg atoms in green and the Cu atoms in orange. For every cluster with 3 SIAs or more, the variant with the lowest energy found within DFT in Fe is represented.

Amas d'interstitiels dans Fe-α

Migration

• n < 4 :

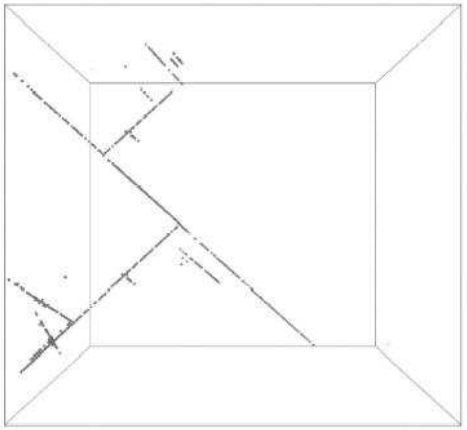

- migration dans la direction <111> (E_m < 0.1eV)
- changement de direction par activation thermique

(E_{a2I}= 0,09eV et E_{a3I}= 0,27eV)

migration 1D/3D

Trajectoire d'un tri-interstitiel dans du fer-α à 1000K

• n ≥ 4 :

glissement 1D dans la direction <111>

➔ migration 1D

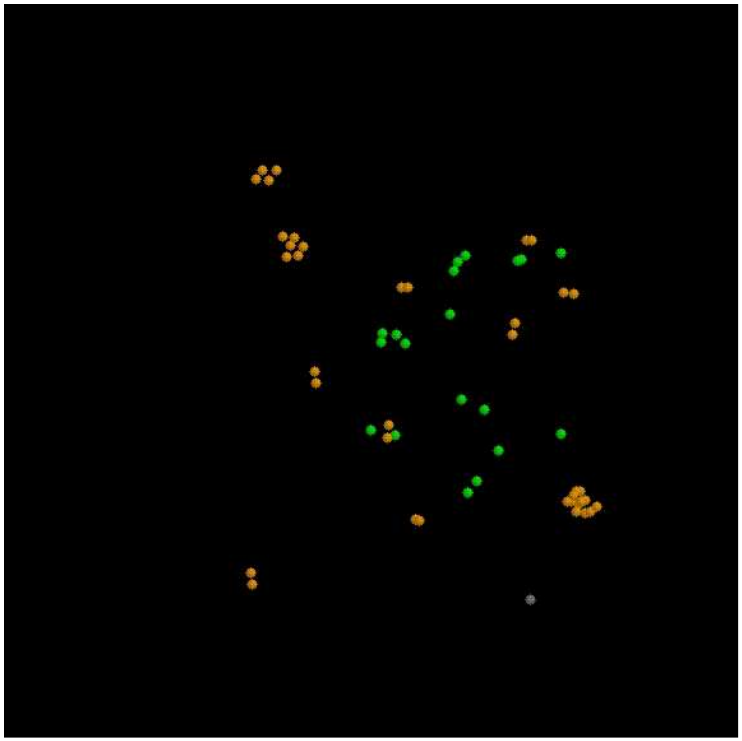

CEA Saclay

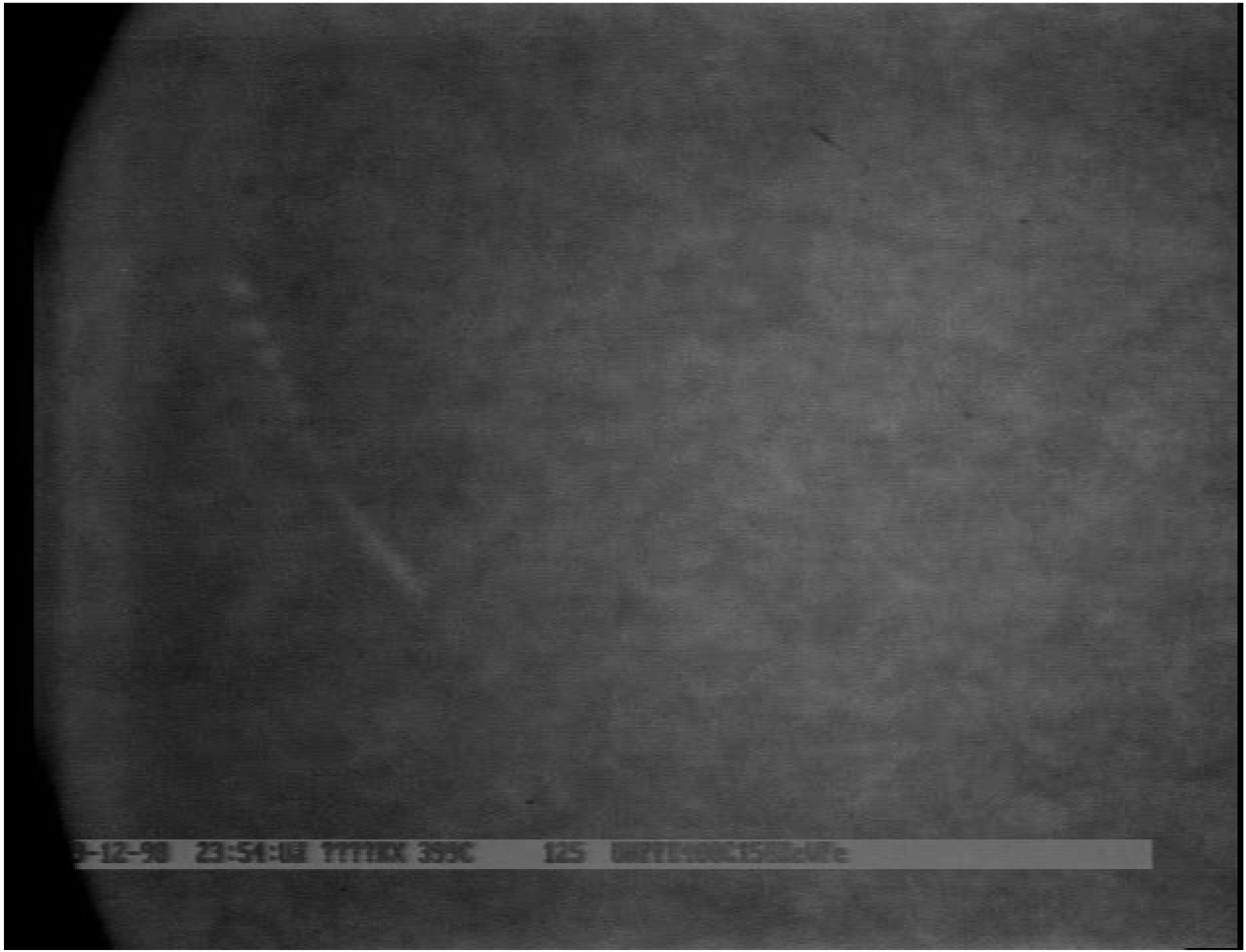

Amas d'interstitiels dans Fe-α

Migration

		E_m (eV)	D_0 ($cm^2.s^{-1}$)
Marian		$0,059 + 0,067 / n^{1,3}$	$8,98.10^{-3}\ n^{-0,61}$
Soneda		0,061	$4,6.10^{-4}$
Bacon		0,022-0,026	-
Wirth	n=19	0,023	$1,7.10^{-3}$
	n=37	0,052	$6,5.10^{-3}$
Osestky		0,02-0,05	-
Kuramoto n=200		0,2	-

⇒ n=20 17cm < x < 68cm pendant 14 jours à 20°C

⇒ n=200 0,95cm < x < 33cm pendant 14 jours à 20°C

Outline

Interaction ion-matter

Ballistic Damage (primary damage)
- Frenkel pairs
- Atomic Displacement Cascade
- Disorder induced by ballistic damage

Properties of point defects and their clusters :
- Structure
- Mobility

Slow evolution (secondary damage) :
- Evolution of the point defects population:
- Consequence of the super-saturation of point defects
  - Agglomeration of point defects
  - Enhanced phase transformation
  - Induced Segregation and precipitation

Macroscopic Consequences

Evolution de la population de défauts ponctuels
Mécanismes fondamentaux

- **Recombination**

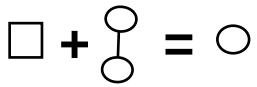
(annihilation)

Recombination rate: $K_{iv} = 4\pi r_{iv} (D_i + D_v) \sim 4\pi r_{iv} D_i = R D_i$

- **Elimination on sinks**
  - grain boundaries,
  - free surfaces,
  - dislocation lines,
  - interfaces …

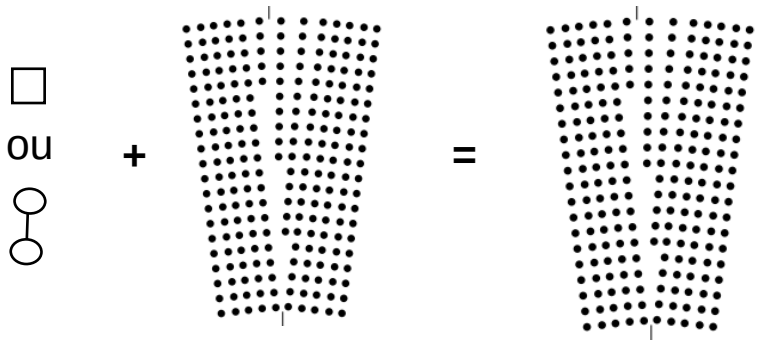

interstitials: i +s = s

$K_{is} = 4\pi r_{is} D_i$

vacancies: v +s = s

$K_{vs} = 4\pi r_{vs} D_v$

Evolution de la population de défauts ponctuels

Classical mean field approach

(cinétique chimique homogène, rate equation, etc.)

1/ True environment

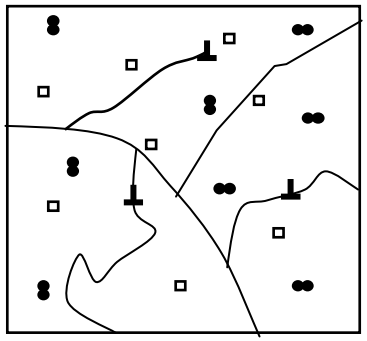

Homogeneous chemical kinetic

Homogeneous environment

c_i, c_v

uniformly absorbing environment

K_v, K_i, R_{iv}

/ Isotrop system for the diffusion as in cubic structures
/ Constant concentration of sinks
/ Vacancies equilibrium concentration neglected

The homogeneous system is characterised by absorption coefficients where index j characterise the nature of the absorbing object

Equation bilan

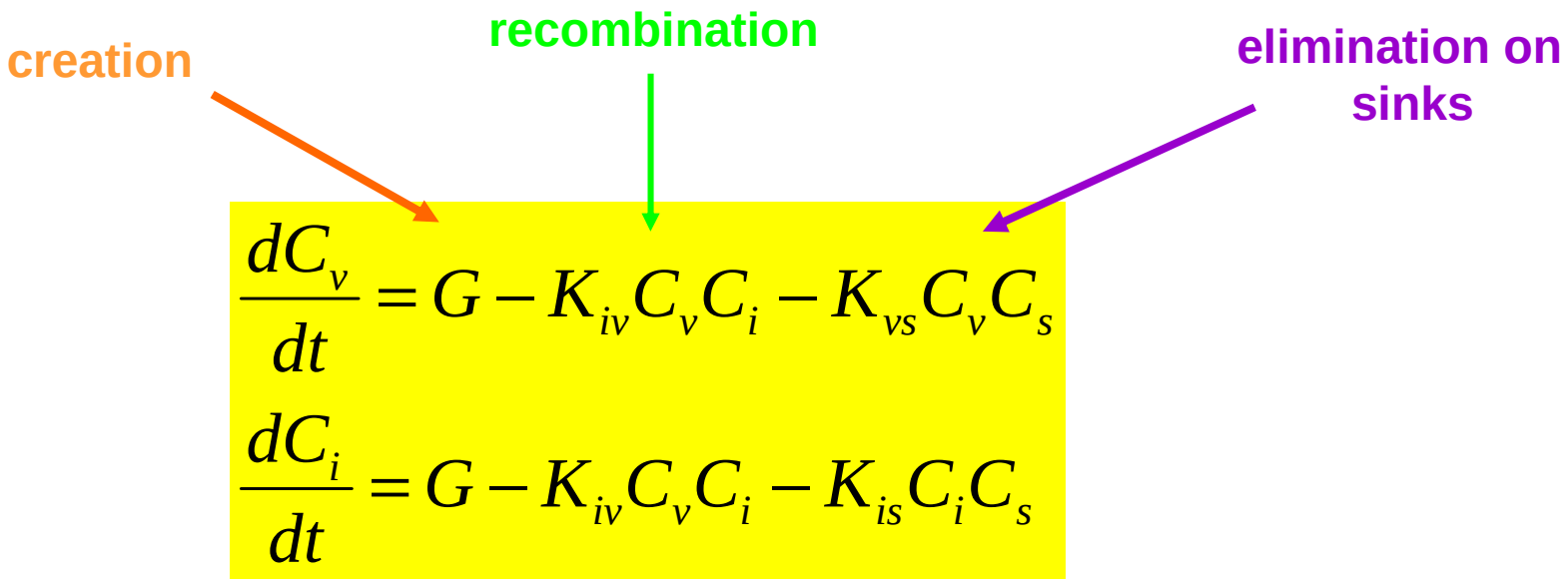

$$\frac{dC_v}{dt} = G - K_{iv}C_vC_i - K_{vs}C_vC_s$$

$$\frac{dC_i}{dt} = G - K_{iv}C_vC_i - K_{is}C_iC_s$$

or (equivalent to)

$$\frac{dC_v}{dt} = G - R\,D_iC_vC_i - K_vD_vC_v$$

$$\frac{dC_i}{dt} = G - R\,D_iC_vC_i - K_iD_iC_i$$

where $K_{vs}\,C_s = K_v\,D_v$

$K_{is}\,C_s = K_i\,D_i$

with $K_\theta = \sum_s k_{\theta s}^2$

$k_{\theta s}^2$ = strength of sink s on defect θ

Elimination on sink

The rate of elimination of point defects (DP) of α type on sink j
is written when diffusion is the controlling process (not reaction at interface)

$$\left.\frac{\partial c_\alpha}{\partial t}\right|_j = -k^2_{j,\alpha} D_\alpha c_\alpha$$

sink strength k^2_j of an object j is given by $k^2_{j,\alpha} = Z_{j,\alpha} Q_j$

Q_j capture rate

$Z_{j,\alpha}$ biais factor depend on the nature of PD

Damask, Wiedersich, Brailsford, Bullough, Nichols

Expression of coefficients

Z is the bias factor (simple way to take into account the interaction)

Z=1 if no interaction taken into account

sink	Q	$Z_{n,\alpha}$
cavity	$4\pi r_c N_c Z_{c,\alpha}$	$Z_{c,i} = Z_{c,v} = 1$
Dislocation loop	$4\pi r_b N_b Z_{b,\alpha}$	$Z_{b,\alpha} = \frac{\pi}{\ln(8r_b / r_{p,\alpha})}$
dislocation	$\rho_d Z_{d,\alpha}$	$Z_{d,\alpha} = \frac{2\pi}{\ln\left\{1/\left[r_{p,\alpha}(\pi\rho_d)^{1/2}\right]\right\}}$
Grain boundary	$\frac{57.6}{d^2}$	$Z_{gb,\alpha} = k'_\alpha d / 9.6$

Also, for Dislocations and dislocation loops : $Z_d^i > Z_d^v$

there is a stronger interaction for interstitial than vacancy because r_p is ~ $V_i^r > V_v^r$

$Z_d^i \approx 1.1 ; 1.2$

commonly used: $Z_d^v \approx 1$

Cavities, grain boundaries and surfaces are neutral sinks (at first order): $Z^i = Z^v = 1$

évolution de la population de défauts ponctuels

Low temperatures and low density of sinks

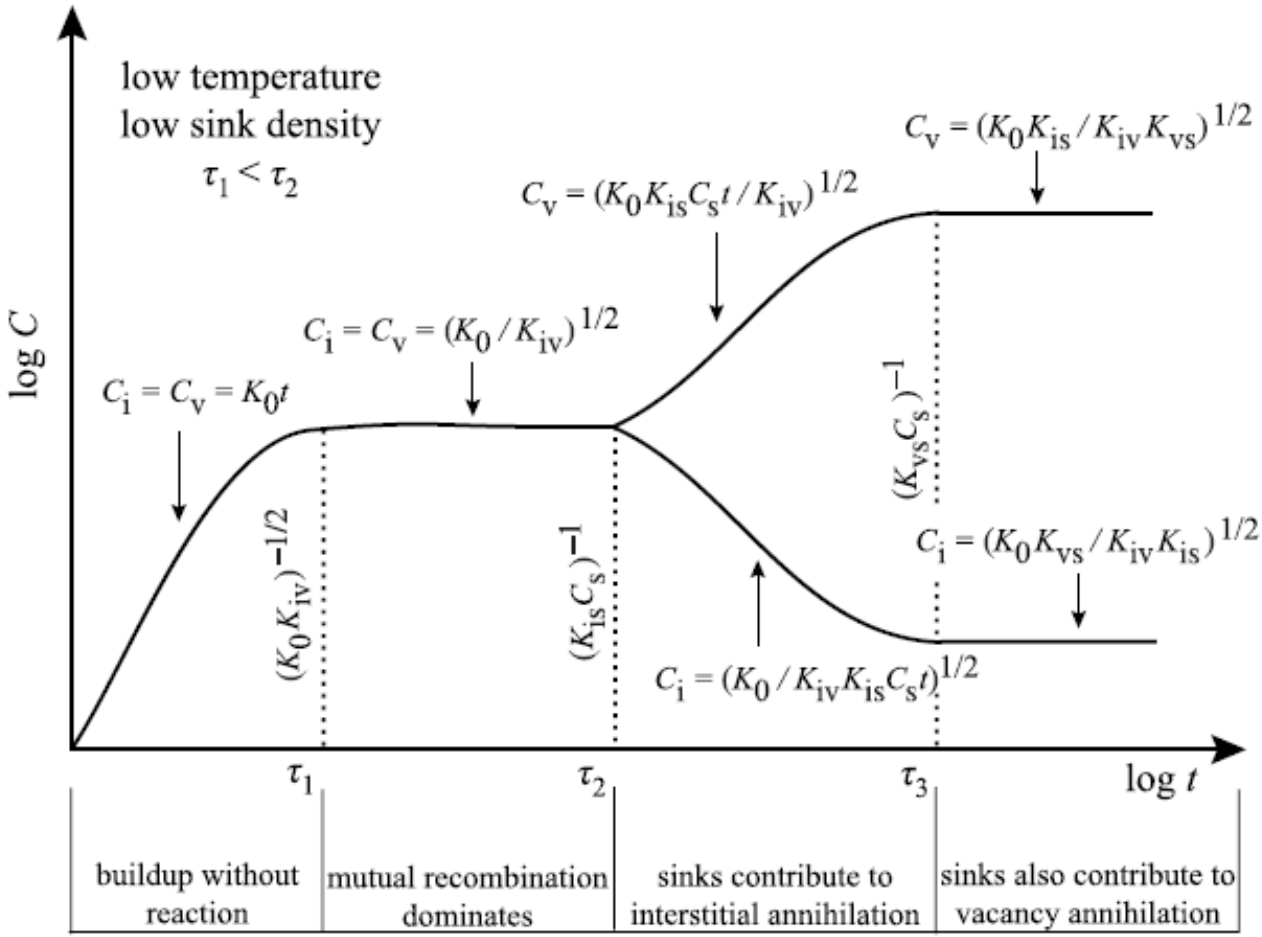

Livre G. Was

évolution de la population de défauts ponctuels

Low temperatures and intermediate density of sinks

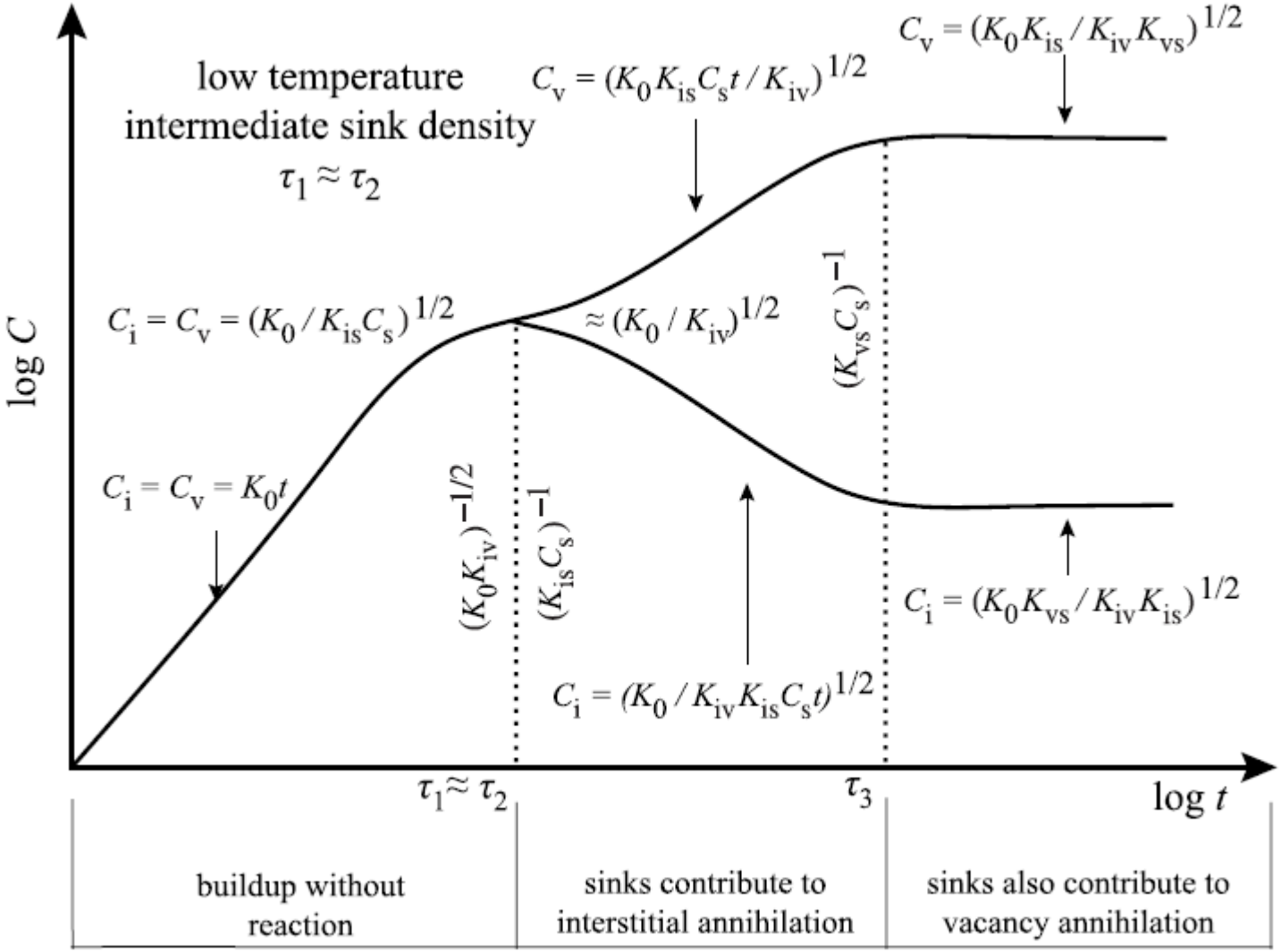

$G = K_0$

Livre G. Was

évolution de la population de défauts ponctuels

Low temperatures and high density of sinks

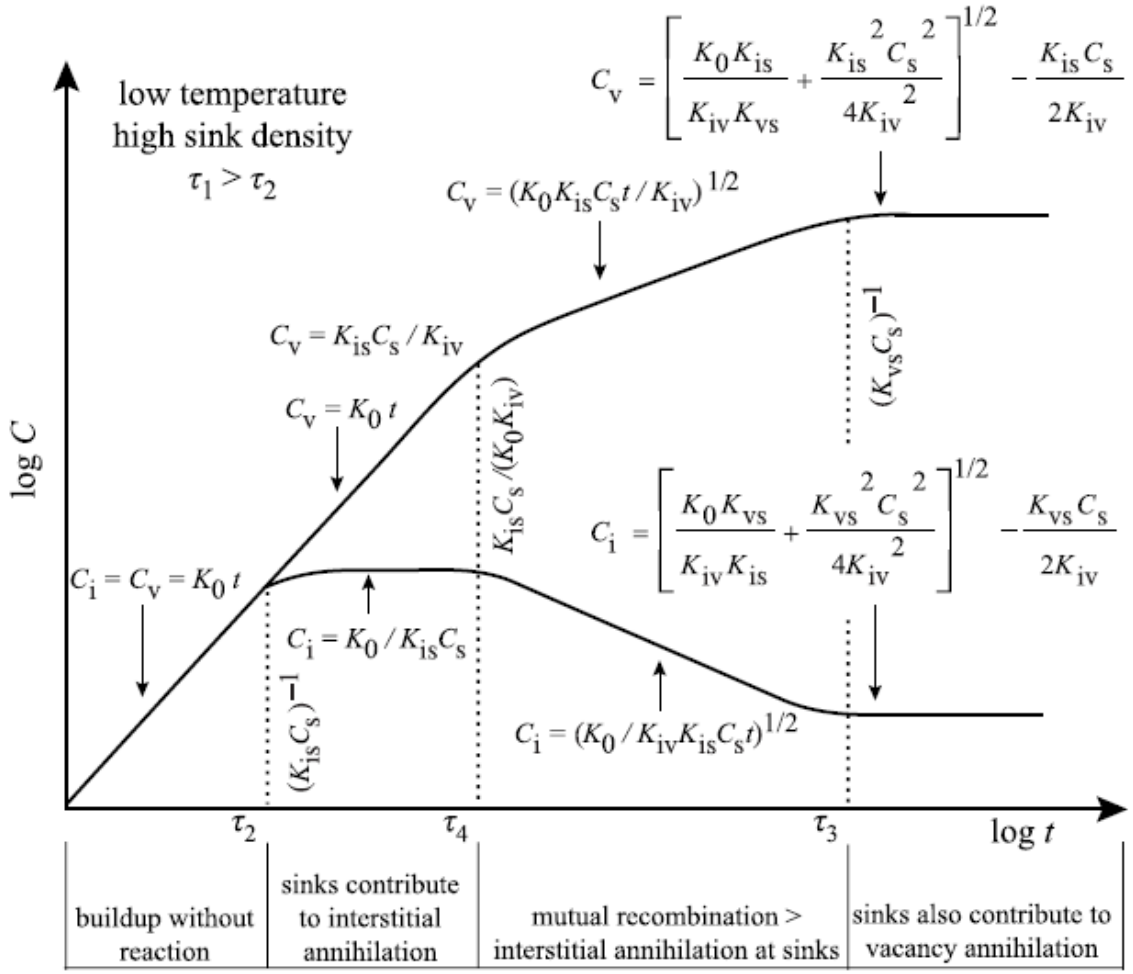

$G = K_0$

Livre G. Was

évolution de la population de défauts ponctuels

High temperatures

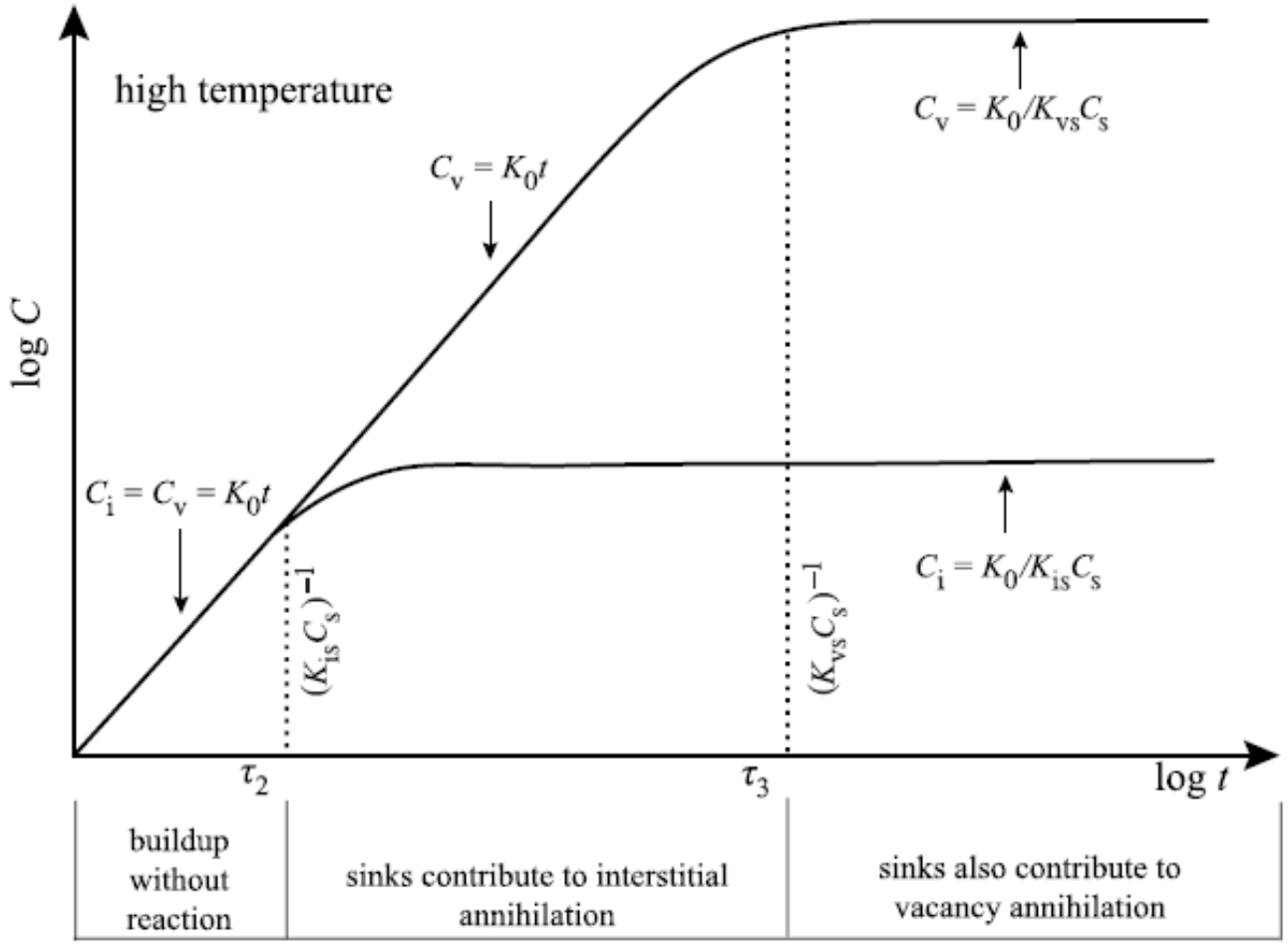

$G = K_0$

Livre G. Was

Examen…

Calculez τ_3 dans le cas d'un réacteur à eau pressurisée
Hypothèse: on suppose que les puits sont majoritairement des dislocations avec $\rho=10^9 cm^{-2}$.

Correction…

$K_v^d = \rho Z_v^d = \rho$

$$\tau_3 = 1/(3.510^{-12} * 10^9) = 285s$$

Court en comparaison de la durée de vie…

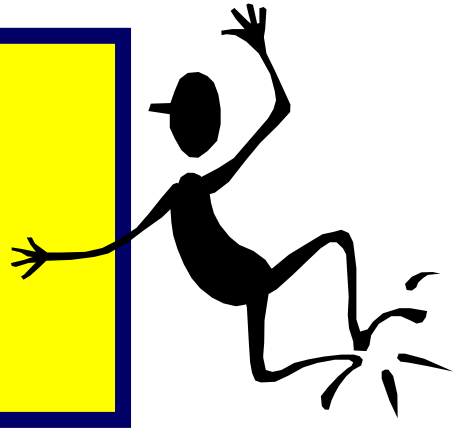

Point defect concentration versus temperature

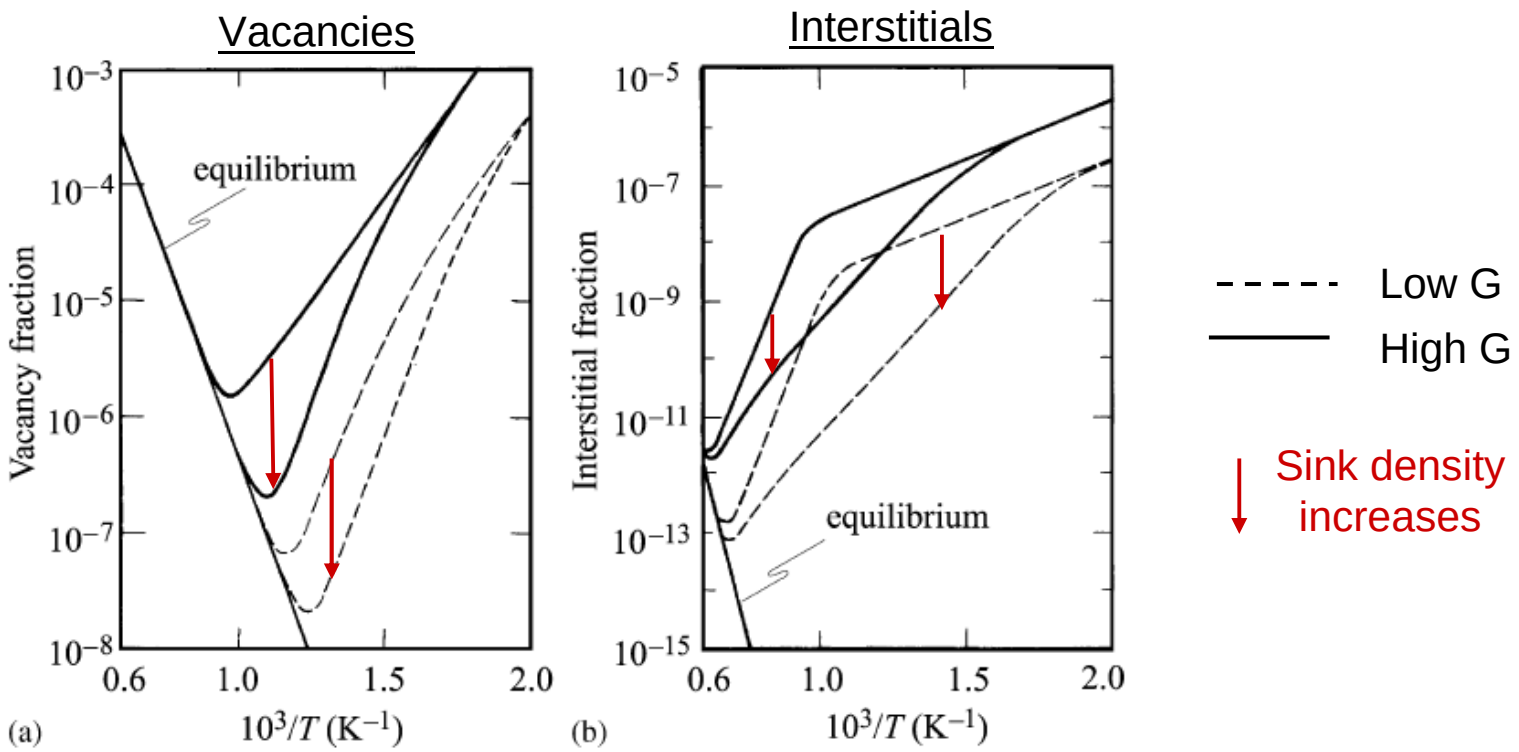

Three domains of temperature may be define:

High temperature — **no irradiation effect** — $C_\theta = C_\theta^{eq}$

Intermediate temperature — **Elimination on sink dominant** — $c_v = \frac{G}{K_v D_v}$ — $c_i = \frac{G}{K_i D_i}$

Low temperature — **Recombination dominant** — $c_v = \left(\frac{G K_i}{R K_v D_v}\right)^{1/2}$ — $c_i = \left(\frac{G K_v D_v}{R K_i D_i^2}\right)^{1/2}$

Défauts étendus (amas de défauts ponctuels)

- **Agglomeration ➔ defect clusters**

Interstitials (SIA) **Dislocation loops (2D)**

dislocation loops in Ni

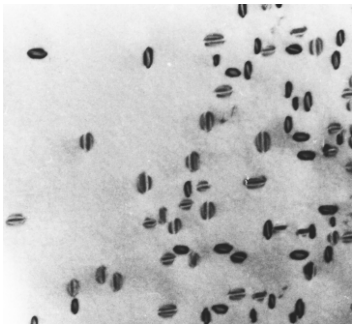

- Frank loops

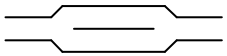

- Perfect loops

Vacancies **Dislocation loops (2D)**

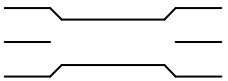

Cavities (3D)

Cavity in Cu

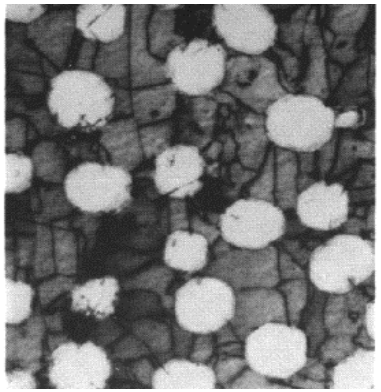

Staking Fault Tetrahedra (3D)

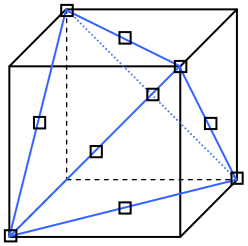

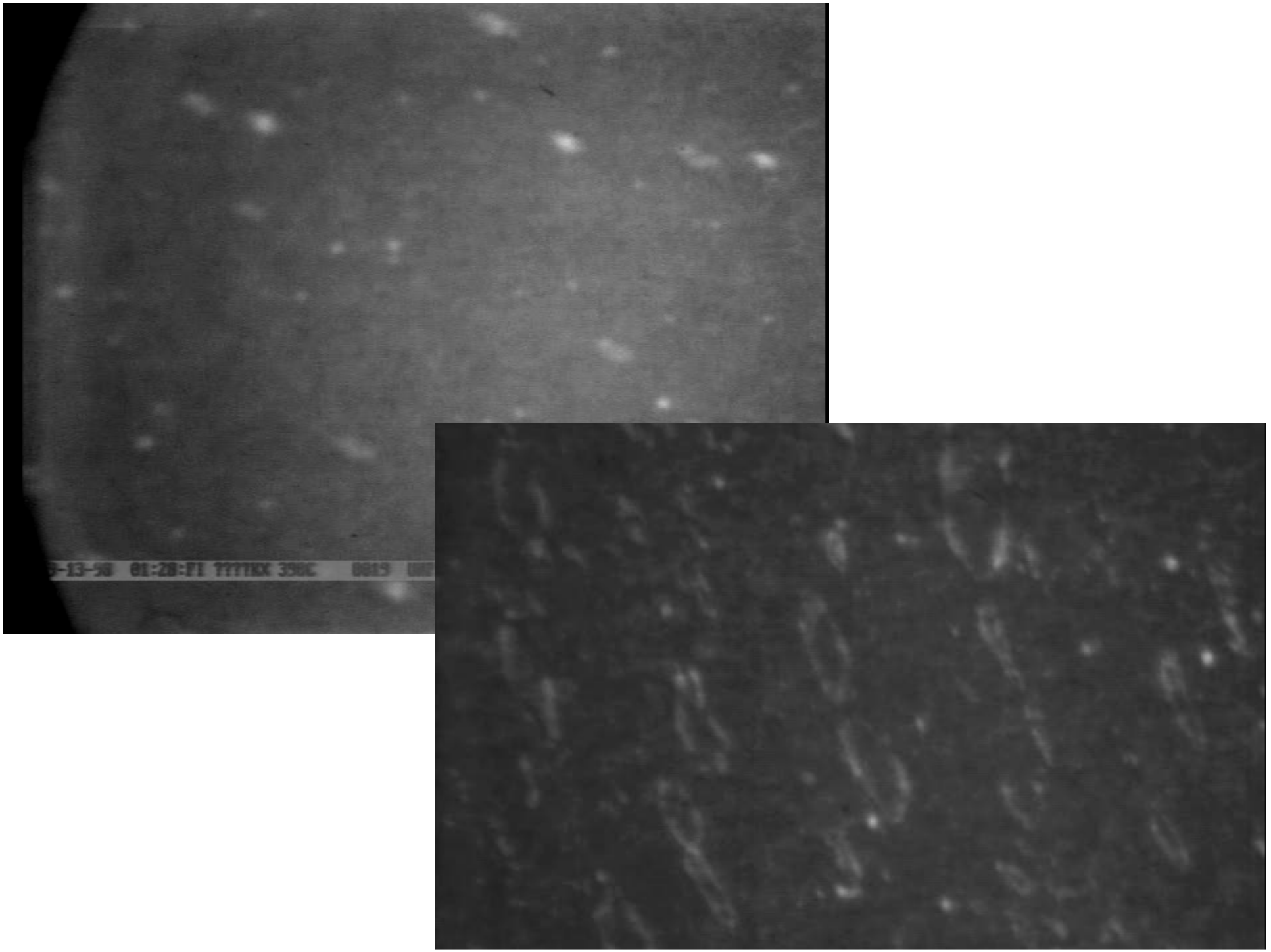

Extended Point defects Clusters

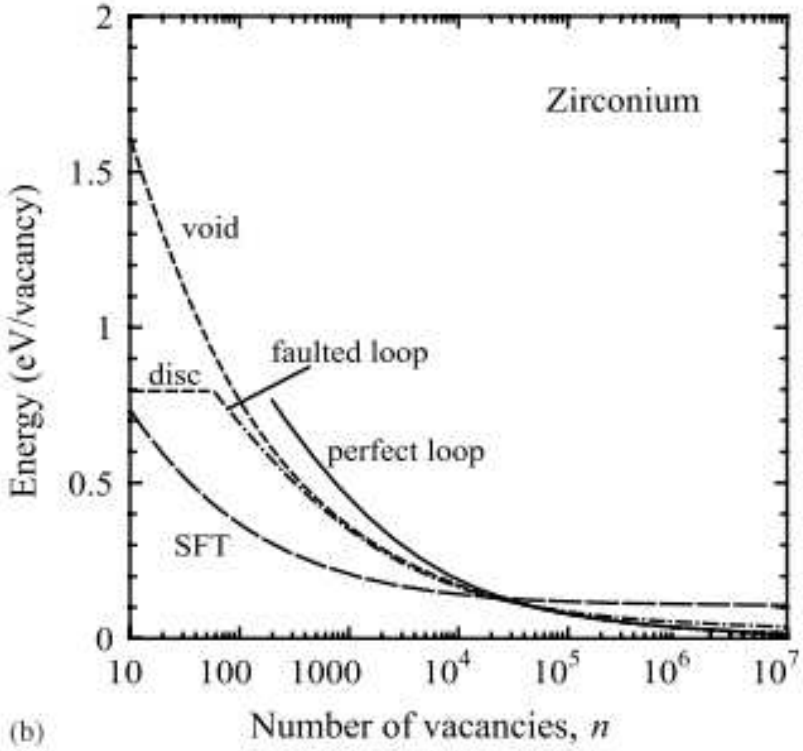

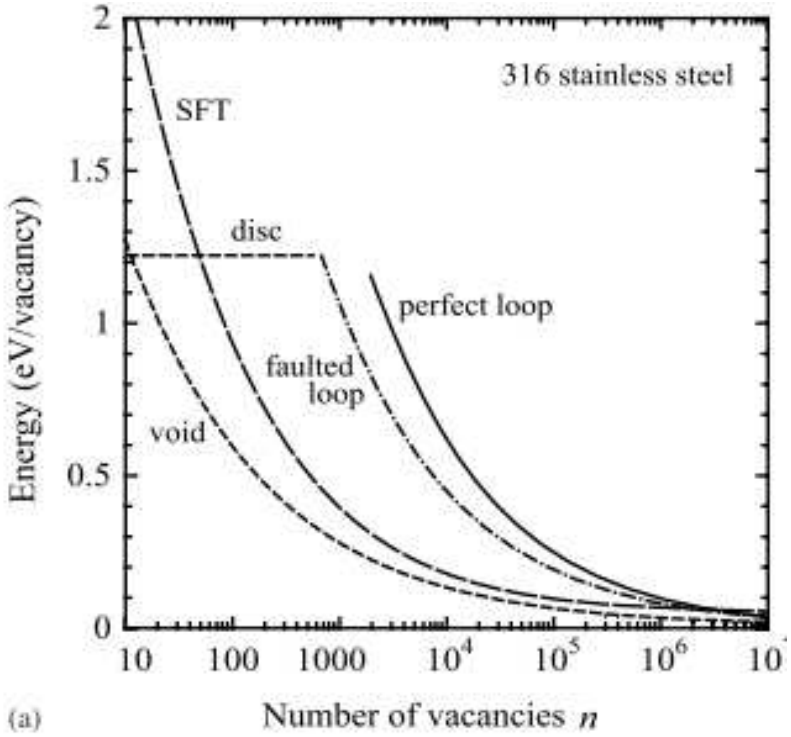

Livre G. Was

Evolution of point defects clusters

Classical mean field approach

True environment

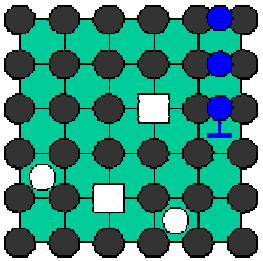

Homogeneous medium

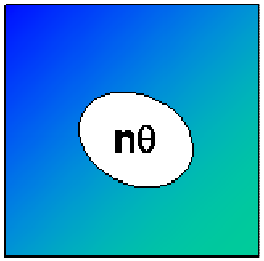

θ = i or v

Consider reactions between clusters

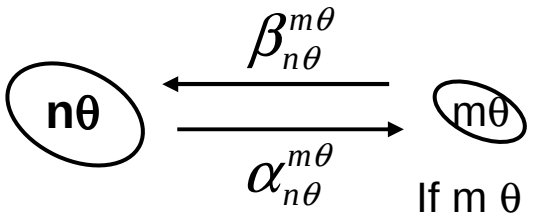

If m θ mobile

General equations *(hypo: only monomers are mobile)*

monomères

$$\frac{dC_{1\theta}}{dt} = G_{1\theta} + \beta_{2\theta}^{1\theta'} C_{2\theta} C_{1\theta'} + 4\alpha_{2\theta}^{1\theta} C_{2\theta} + \sum_{n=3} (\alpha_{n\theta}^{1\theta} C_{n\theta}) - \sum_{n=2} (\beta_{n\theta}^{1\theta} C_{n\theta} + \beta_{n\theta}^{1\theta'} C_{n\theta'}) C_{1\theta} - 4\beta_{1\theta}^{1\theta} C_{1\theta} C_{1\theta} - R_{iv} C_{1\theta} C_{1\theta'} - K_{1\theta}^{d} (C_{1\theta} - C_{1\theta}^{eq}) - K_{1\theta}^{sk} (C_{1\theta} - C_{1\theta}^{eq})$$

dimères

$$\frac{dC_{2\theta}}{dt} = G_{2\theta} + 2\beta_{1\theta}^{1\theta} C_{1\theta} C_{1\theta} + \beta_{3\theta}^{1\theta'} C_{1\theta'} C_{3\theta} + \alpha_{3\theta}^{1\theta} C_{3\theta} - 2\alpha_{2\theta}^{1\theta} C_{2\theta} - \beta_{2\theta}^{1\theta} C_{1\theta} C_{2\theta} - \beta_{2\theta}^{1\theta'} C_{1\theta'} C_{2\theta}$$

n>2

$$\frac{dC_{n\theta}}{dt} = G_{n\theta} + \beta_{(n-1)\theta}^{1\theta} C_{1\theta} C_{(n-1)\theta} + (\beta_{(n+1)\theta}^{1\theta'} C_{1\theta'} + \alpha_{(n+1)\theta}^{1\theta}) C_{(n+1)\theta} - (\alpha_{n\theta}^{1\theta} + \beta_{n\theta}^{1\theta} C_{1\theta} + \beta_{n\theta}^{1\theta'} C_{1\theta'}) C_{n\theta}$$

Diffusion under irradiation

Diffusion of in pure metal

Theory of diffusion ➔ $D^* = \alpha_v D_v C_v + \alpha_i D_i C_i$ α: correlation factor

- Excepted at high T, $\mathbf{C_v >> C_v^{eq}}$
- Diffusion via **interstitials only occurs under irradiation** (C_i^{eq} ~0)

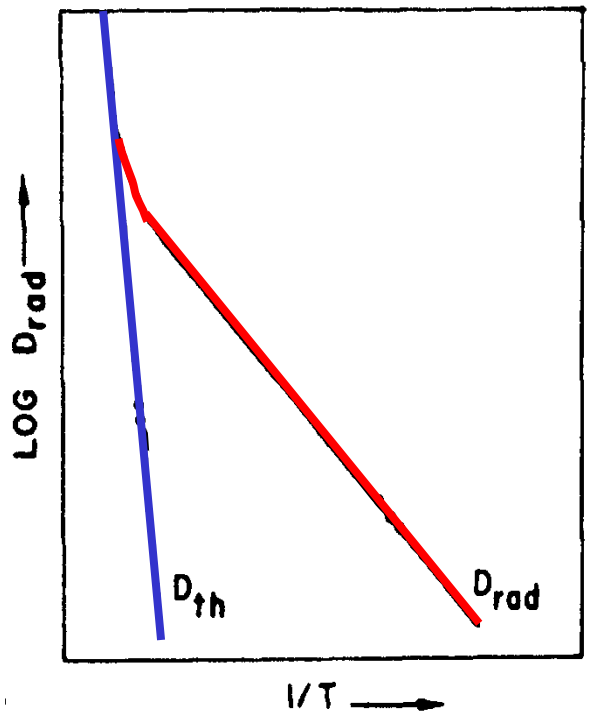

➔ Excepted at high T, **$D^* >> D^{th}$**

= radiation enhanced diffusion

Ex: Cu in irradiated FeCu

$D_{Cu}^{irrad} \approx D_v c_v = 3\ 10^{-12} \times 3\ 10^{-8} = 9\ 10^{-20}\ cm^2/s$

$D_{Cu}^{th} = D_v\ c_v^e = 3\ 10^{-12} \times 8\ 10^{-16} = 2\ 10^{-25}\ cm^2/s$

Irradiation enhanced precipitation

If cross coefficient can be neglected, the only effect of irradiation is to sustain a large defect supersaturation which:

➔ Increase the solute diffusion coefficient

➔ must **not modify the thermodynamic** of the system

⇒ The **precipitation process will be accelerated**
= Irradiation enhanced precipitation

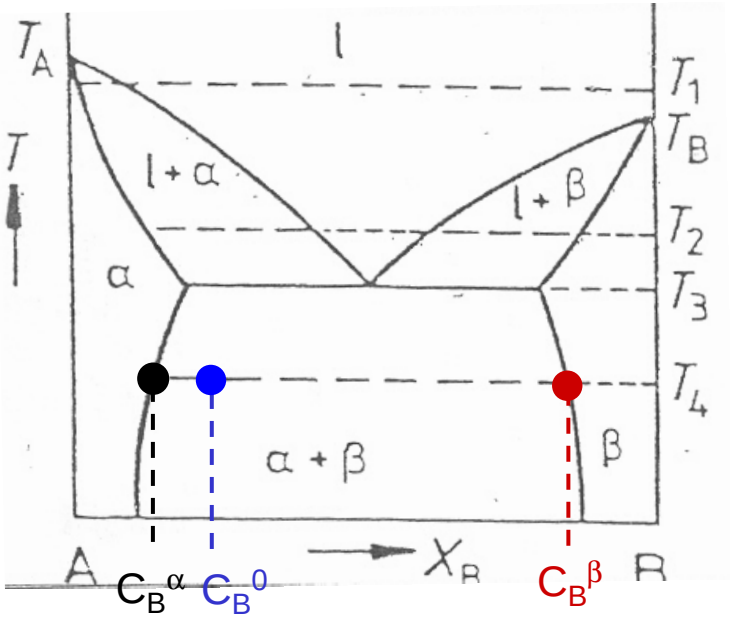

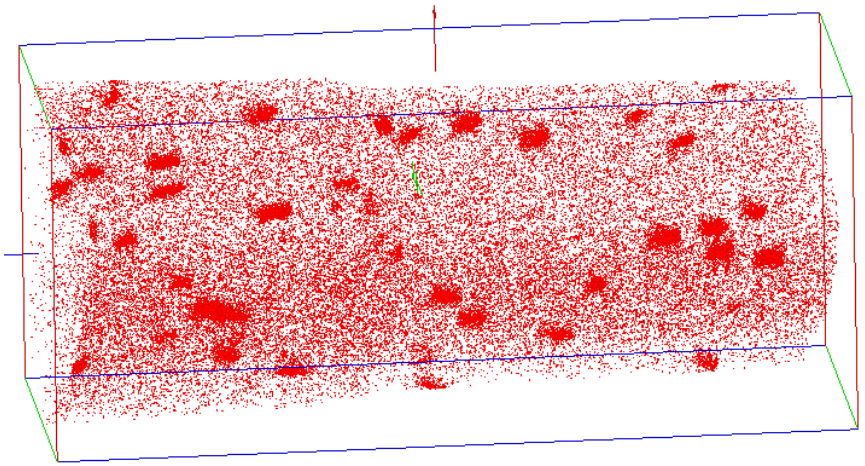

$V = 45 \times 45 \times 100\ nm^3$

Parameters influencing D*

Self-diffusion of Cu

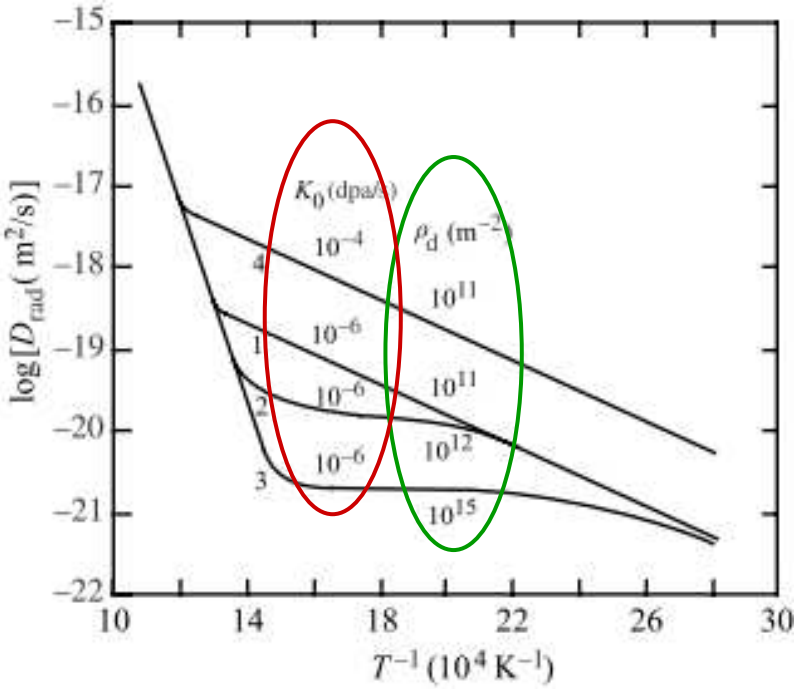

Ni-base irradiated at 10^{-6} dpa.s^{-1}

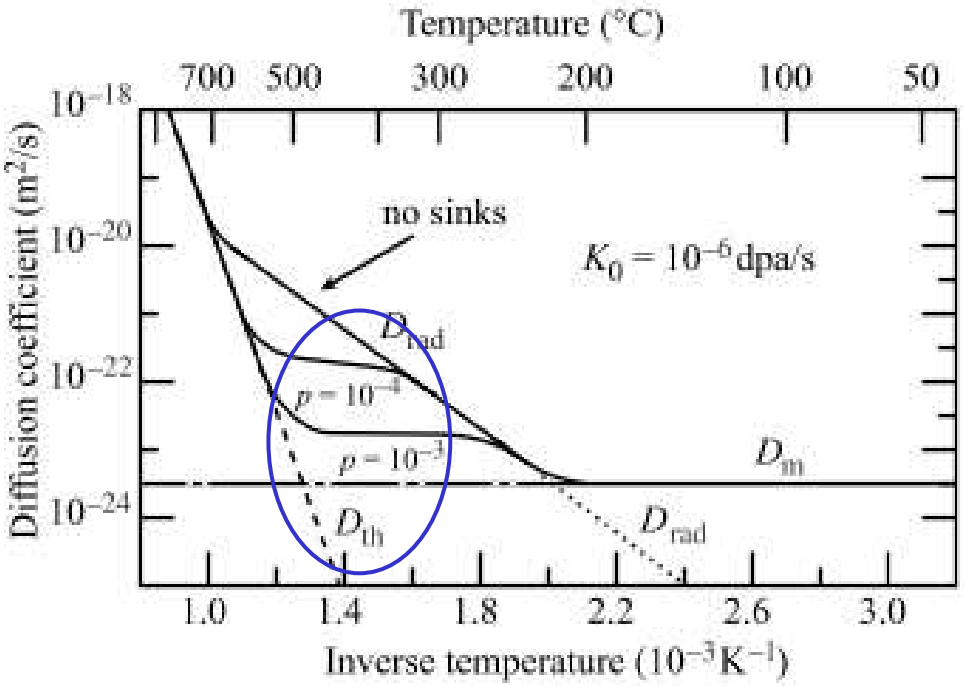

- **Dislocation density** **(concentration of sinks)**
- **Production rate**
- **Sink strength**

Solute transport under irradiation in AB alloy

Mécanismes lacunaire

(avec interaction B-v positive)

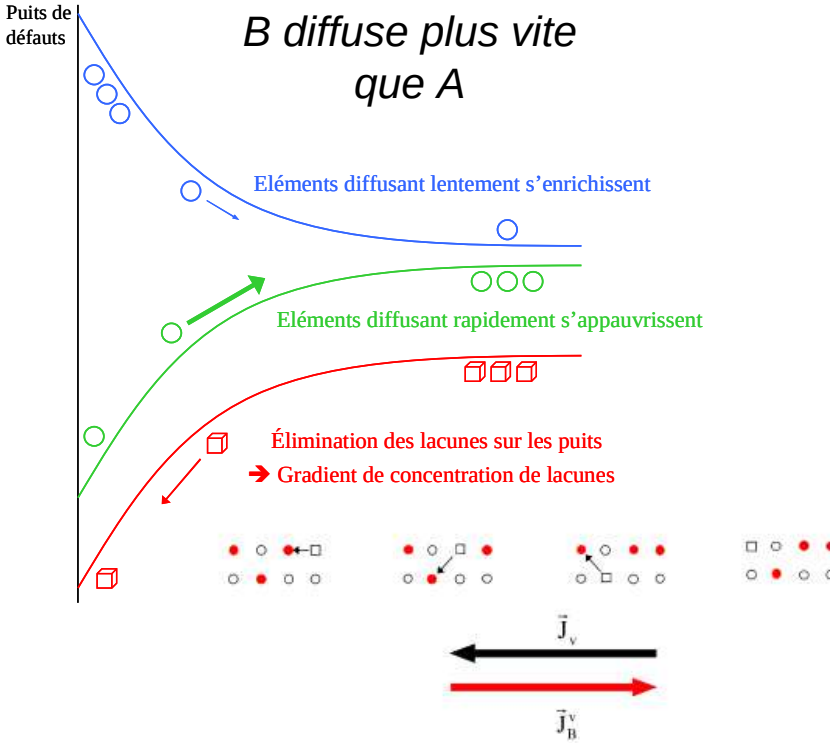

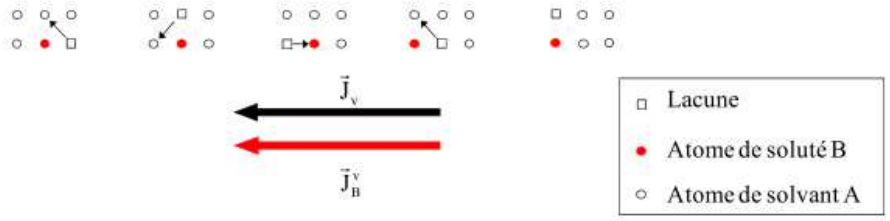

Mécanisme interstitiel

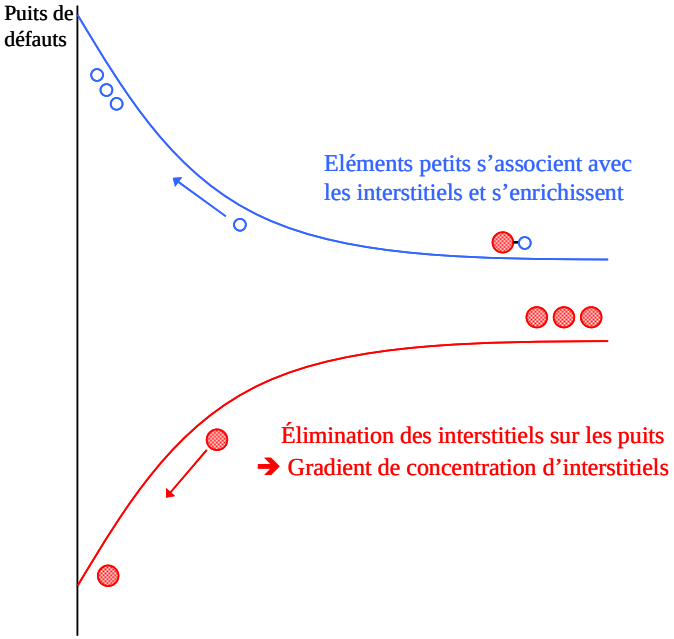

➔ **modification de la concentration locale au niveau du puits de défauts**

$$\frac{\partial c_B}{\partial t} = -div\mathbf{J}_B$$

Solute transport under irradiation in AB alloy

Annihilation of point defects at sinks ➔ **Gradient of concentration**

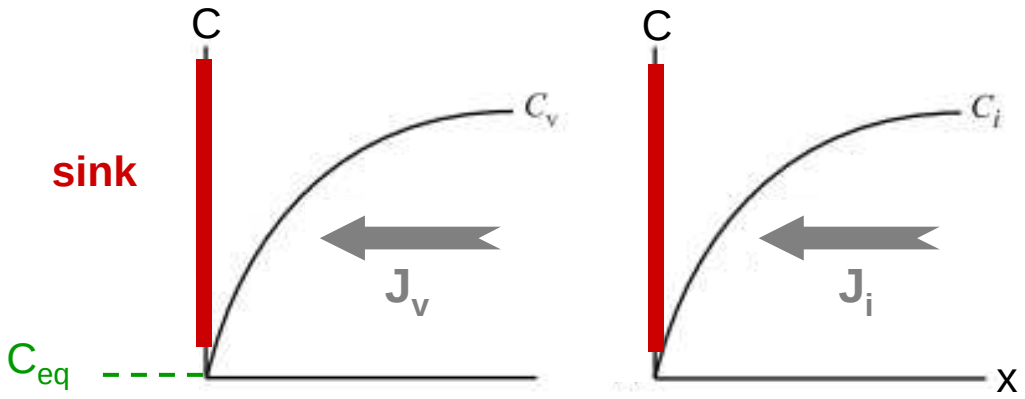

$$\frac{\partial c_i}{\partial t} = G - div\mathbf{J}_i - R\ D_i C_i C_v$$

$$\frac{\partial c_v}{\partial t} = G - div\mathbf{J}_v - R\ D_i C_i C_v$$

➔ **Flux of point defects toward sinks**

By coupling, point defect fluxes result in a **flux of solute atoms** (B)

$$\begin{cases} \mathbf{J}_v = -\left(D_v \nabla c_v + d_{Bv} c_v \nabla c_B\right) \\ \mathbf{J}_i = -\left(D_i \nabla c_i + d_{Bi} c_i \nabla c_B\right) \\ \mathbf{J}_B = -\left(D_B \nabla c_B + c_B \left(d_{Bv} \nabla c_v + d_{Bi} \nabla c_i\right)\right) \end{cases}$$

Zones dénudées au voisinage des joints de grains

- Les zones dénudées en défauts ponctuels se manifestent par l'existence de zones dénudées en boucles.
- Elles n'apparaissent pas pour tous les joints (L'efficacité des joints de grains pour l'élimination des défauts ponctuels dépend de leur nature).

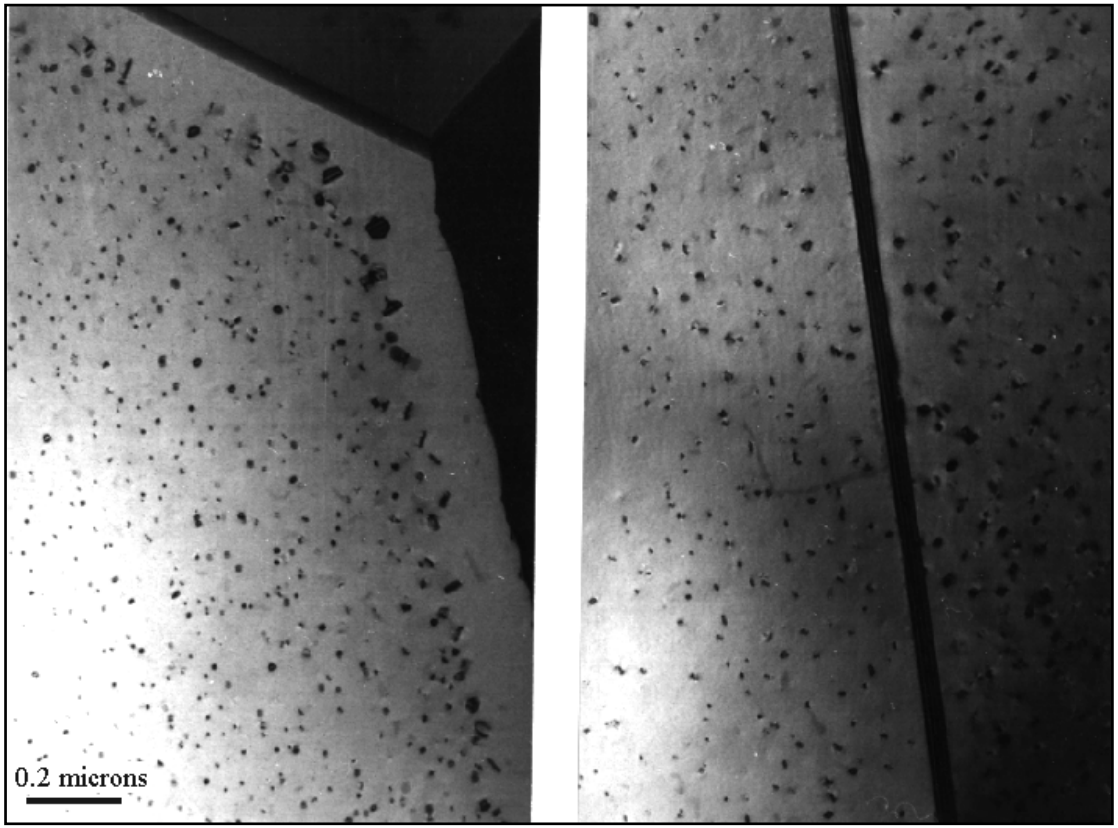

Alliage à base de Nickel irradié avec des électrons de 2 MeV (5 10^{-9} dpa/s, 300°C, 8. 10^{-5}dpa).

FeNiCrSi model alloy : 5 MeV Ni++

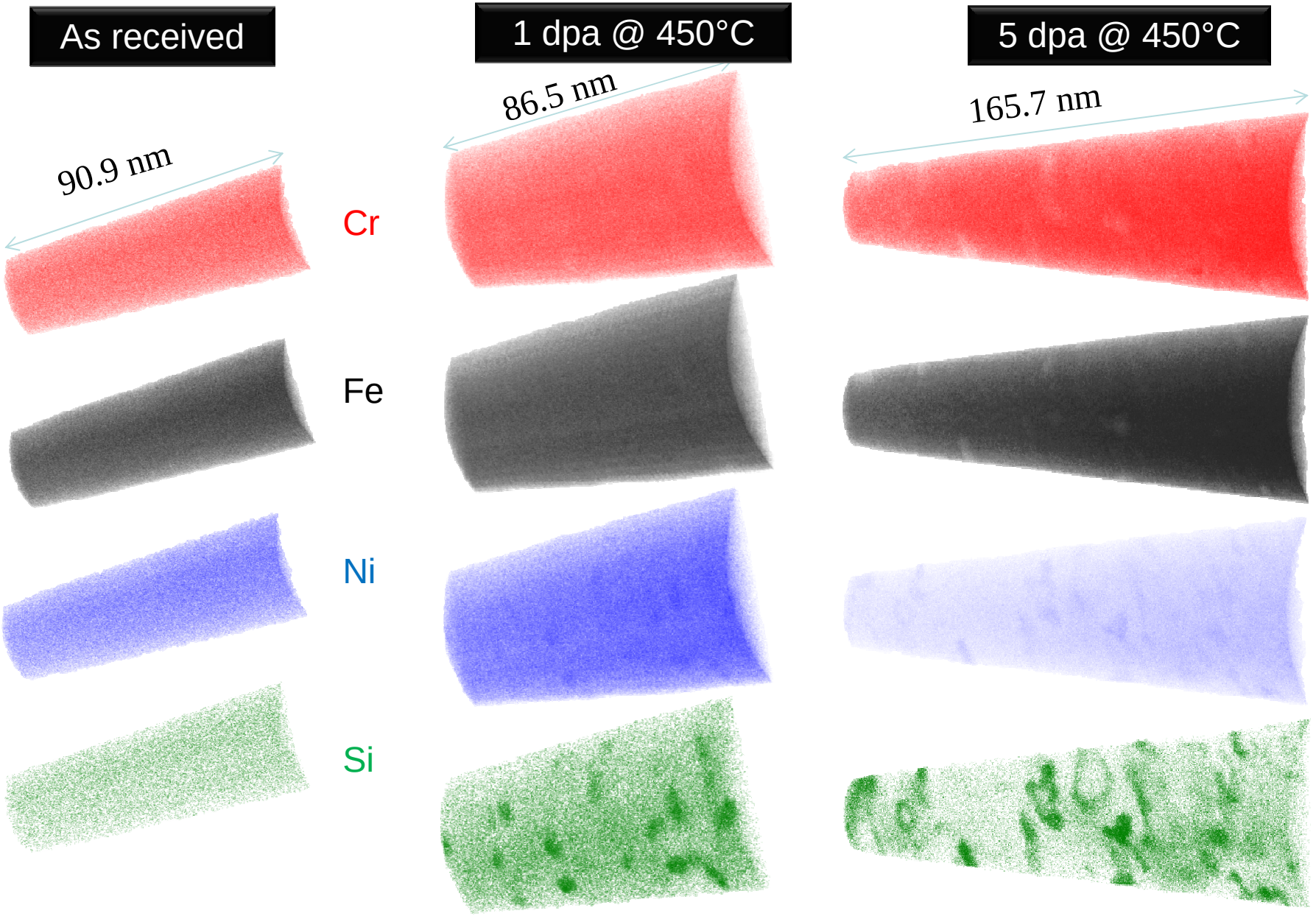

Outline

Interaction ion-matter

Ballistic Damage (primary damage)
- Frenkel pairs
- Atomic Displacement Cascade
- Disorder induced by ballistic damage

Properties of point defects and their clusters :
- Structure
- Mobility

Slow evolution (secondary damage) :
- Evolution of the point defects population:
- Consequence of the super-saturation of point defects
  - Agglomeration of point defects
  - Enhanced phase transformation
  - Induced Segregation and precipitation

Macroscopic Consequences

Chaque Matériau est un cas particulier

Composants et matériaux

- aciers faiblement alliés
- aciers inoxydables
- alliages base nickel
- alliages de zirconium
- alliages divers (Ag-In-Cd)
- céramique (UO2-PuO2)

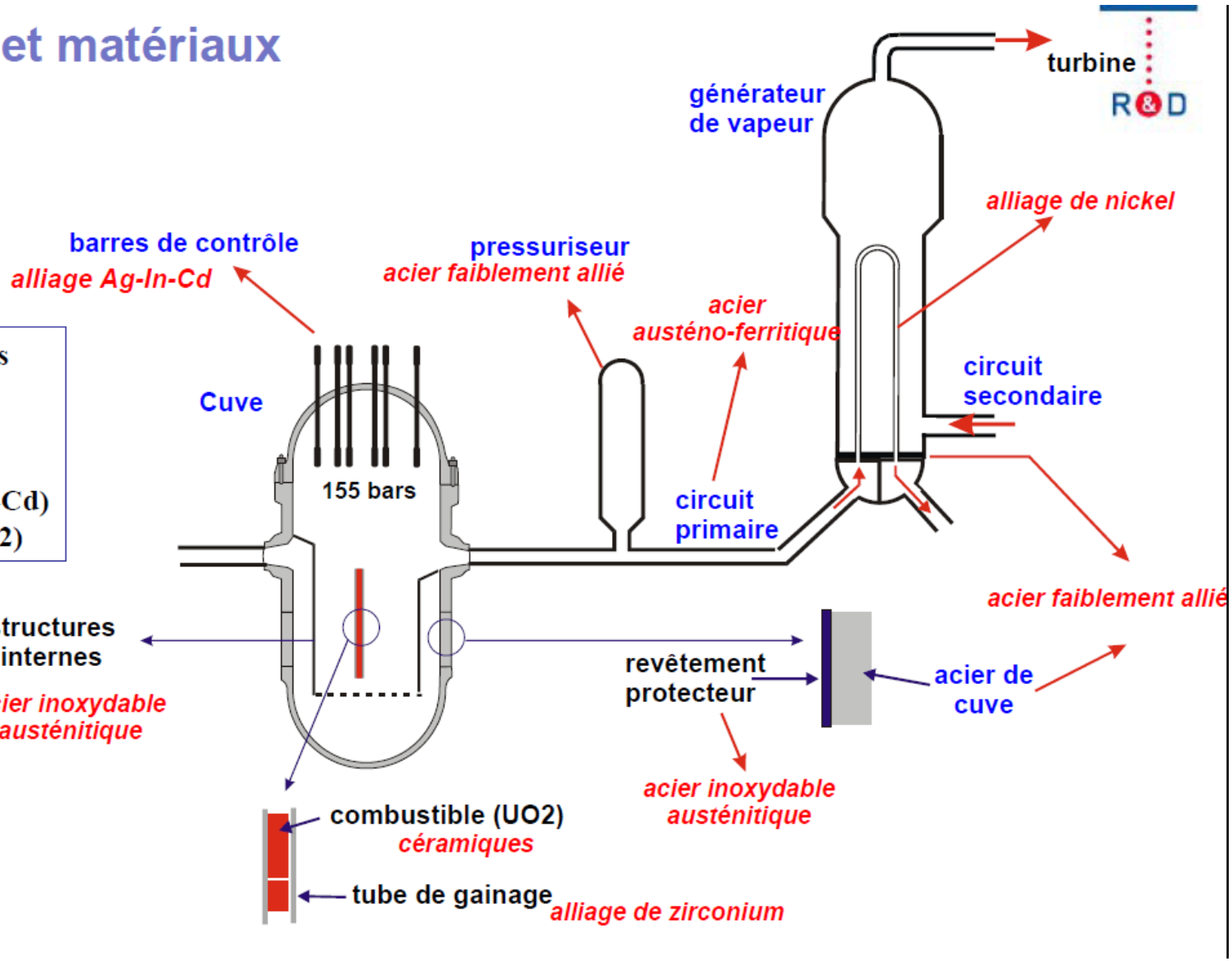

Dimensional variations

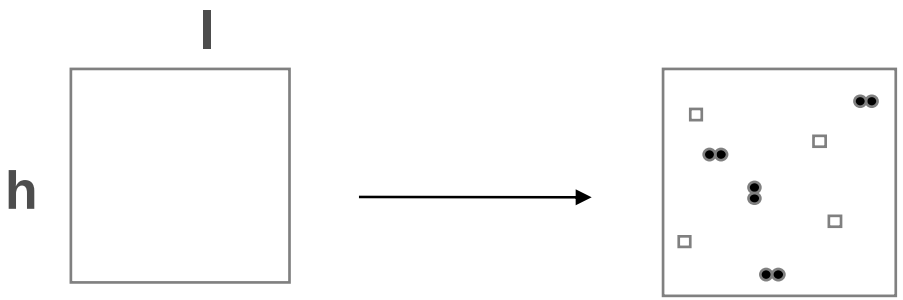

Volume V

V(1+ε)

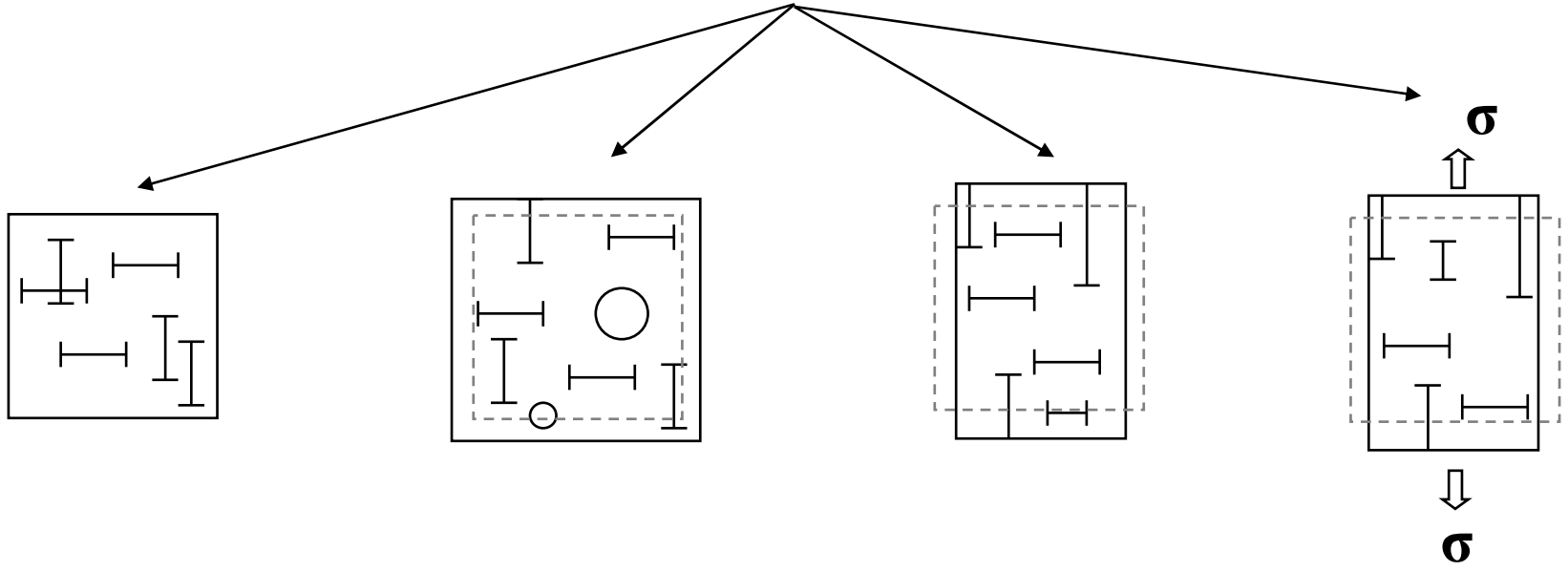

V, h=l

Hardening

V+ΔV, $h_1=l_1$

Swelling

V, h≠l

Growth

V, h≠l

Creep

Swelling

Only happen when the vacancy flux towards cavities
is more important than the interstitial one

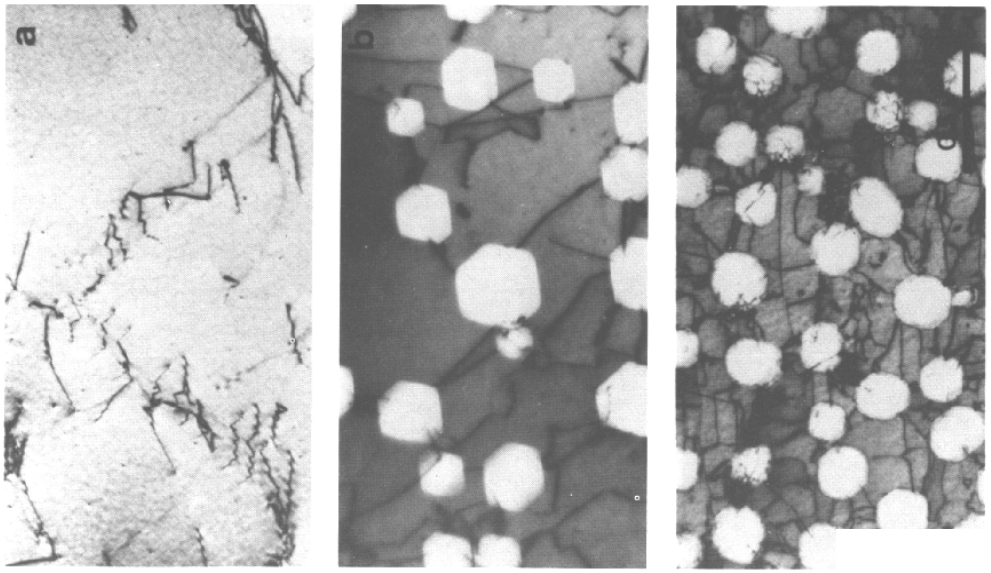

500°C irradiation with Cu ions of 500 keV at 3 10^{-3} dpa/s; Oxygen 30, 70 et 110 ppm (Glowinsky 1976)

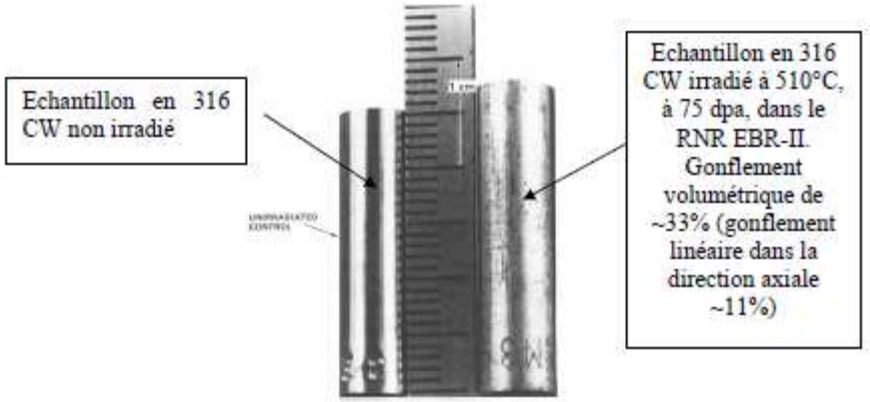

Figure I-20
Gonflement macroscopique de ~33% en volume, et ~11% en linéaire, observé dans un acier de type 316 CW, irradié à 510°C, à 75 dpa dans le RNR EBR-II. L'échantillon à gauche est non irradié et celui de droite est irradié [77].

Hardening

- Increase of the tensile strength
- Decrease of the elongation.

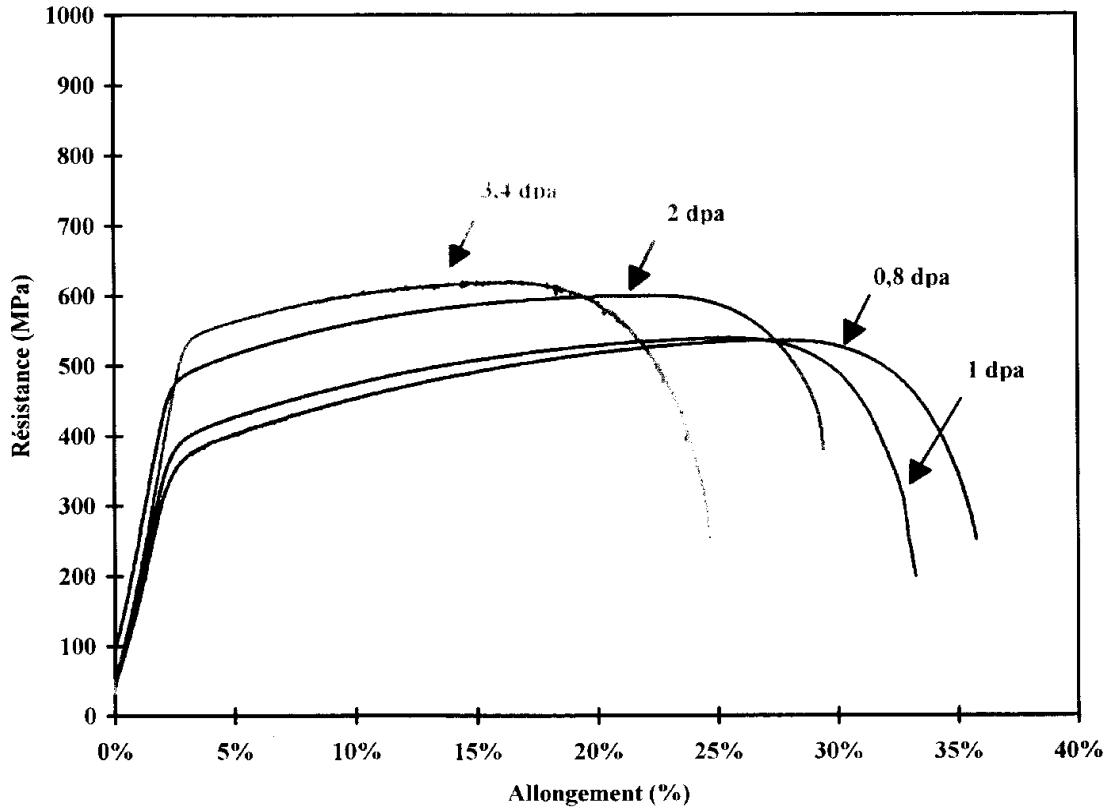

Evolution des courbes de traction d'un acier austénitique (316) irradié avec des neutrons, à 325°C, en fonction de la fluence en dpa.

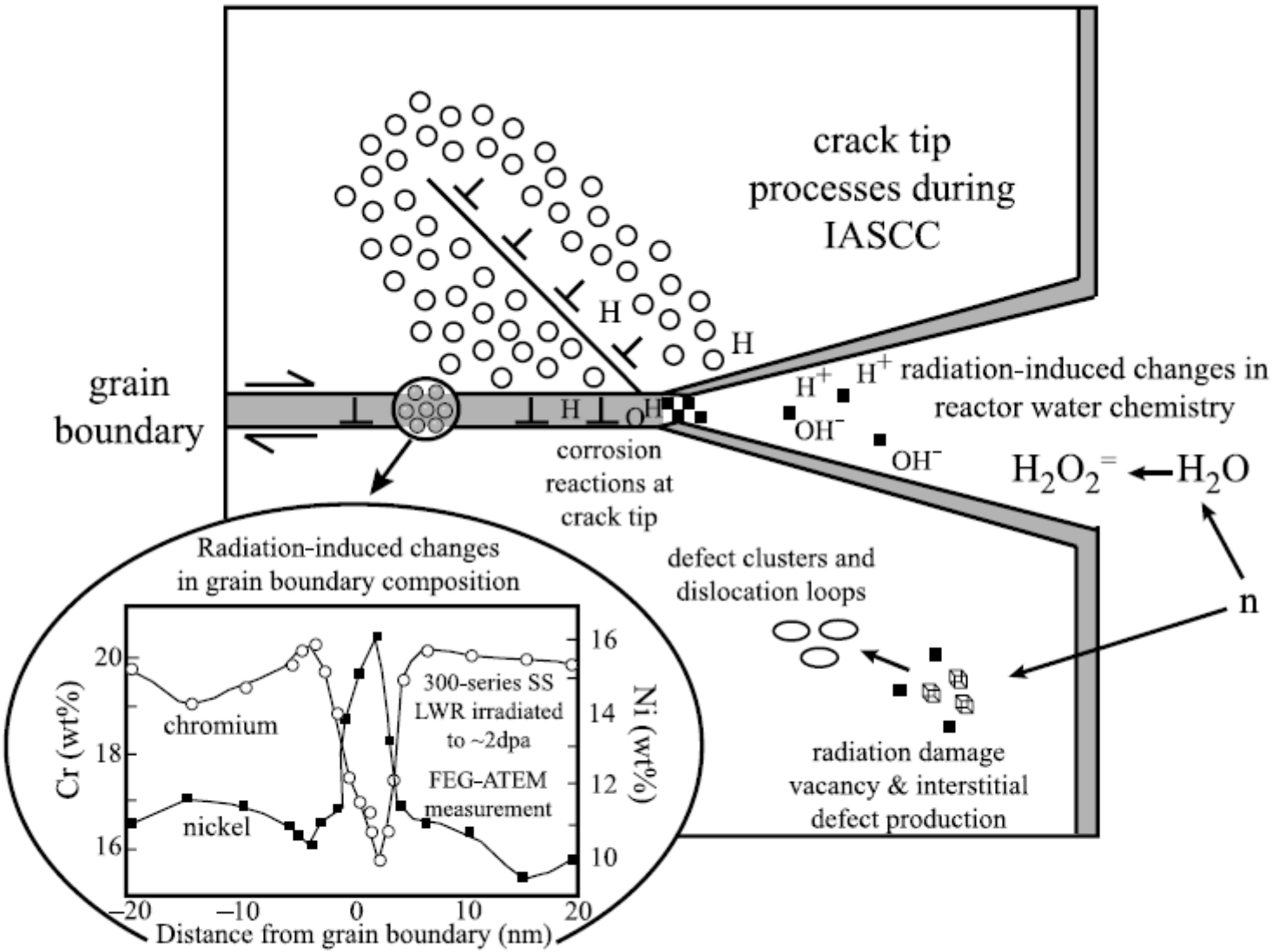

Fig. 15.3. Schematic illustration of mechanistic issues believed to influence crack advance during IASCC of austenitic stainless steels in LWRs (from [6])

EVOLUTION DE LA MICROSTRUCTURE DES METAUX ET ALLIAGES METALLIQUES SOUS IRRADIATION

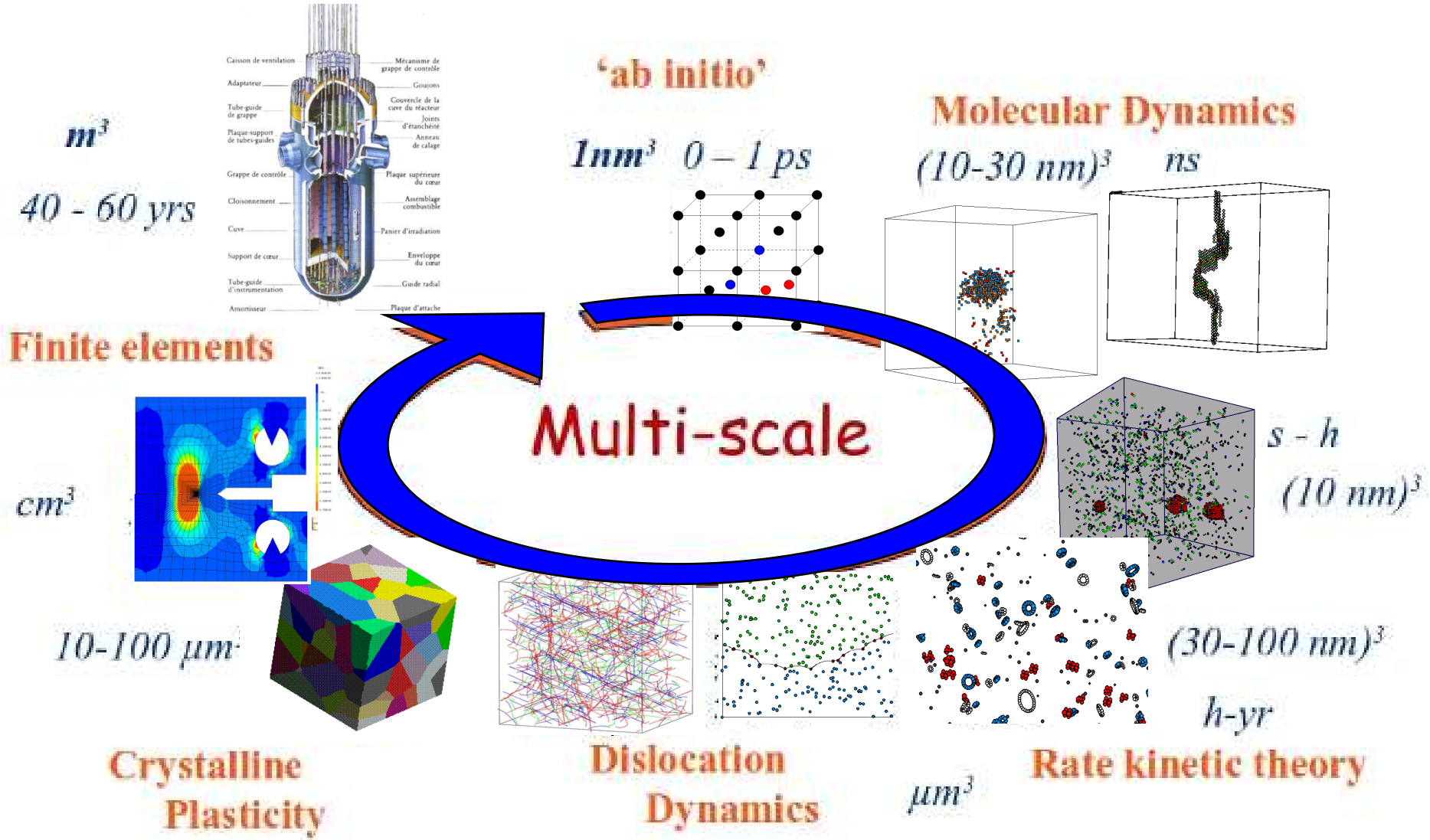

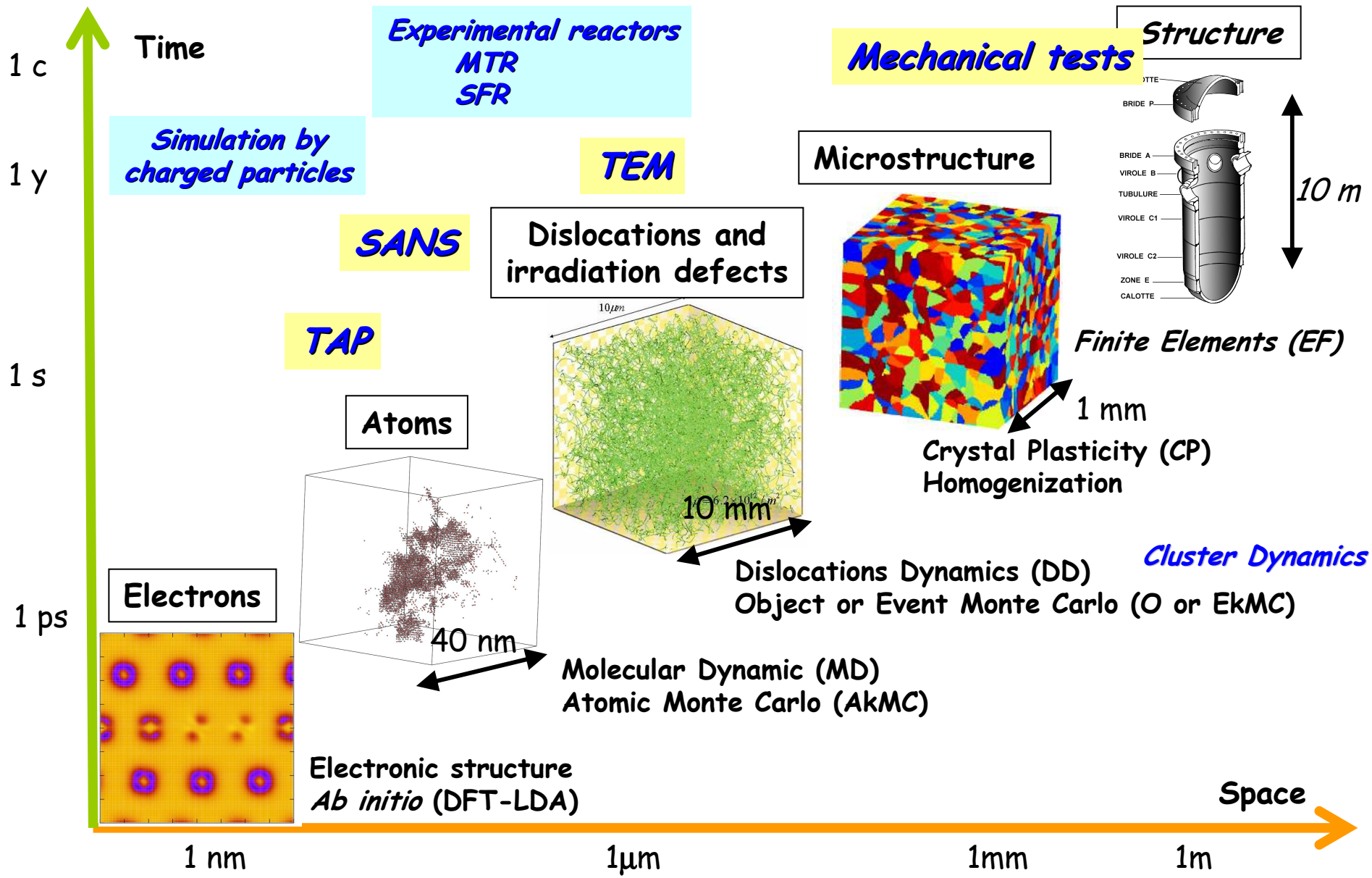
Time
1 c
1 y
1 s
1 ps
Experimental reactors
MTR
SFR
Simulation by
charged particles
TEM
SANS
TAP
Dislocations and
irradiation defects
Microstructure
Structure
Mechanical tests
BRIDE P
BRIDE A
VIROLE B
TUBULURE
VIROLE C1
VIROLE C2
ZONE E
CALOTTE
10 m
Finite Elements (EF)
1 mm
Crystal Plasticity (CP)
Homogenization
Atoms
10 mm
Cluster Dynamics
Dislocations Dynamics (DD)
Object or Event Monte Carlo (O or EkMC)
Electrons
40 nm
Molecular Dynamic (MD)
Atomic Monte Carlo (AkMC)
Electronic structure
Ab initio (DFT-LDA)
Space
1 nm
1µm
1mm
1m